Novel Tacrine-Benzofuran Hybrids as Potent Multitarget-Directed Ligands for the Treatment of Alzheimers Disease: Design, Synthesis, Biological Evaluation, and X-ray Crystallography

SUPPORTING INFORMATION

Novel Tacrine-Benzofuran Hybrids as Potent Multitarget-Directed Ligands for the Treatment of Alzheimer's Disease: Design, Synthesis, Biological Evaluation and X-ray Crystallography

Xiaoming Zha,[a*§] Doriano Lamba,[b§] Lili Zhang,[a,c] Yinghan Lou,[a,d] Changxu Xu,[a,c] Di Kang,[a,d] Li Chen,[c] Yungen Xu,[d] Luyong Zhang,[a] Angela De Simone,[e] Sarah Samez,[b,f] Alessandro Pesaresi,[b] Jure Stojan,[g] Manuela G. Lopez,[h] Javier Egea,[h] Vincenza Andrisano,[d] and Manuela Bartolini [i,*]

[a]*State Key Laboratory of Natural Medicines and Jiangsu Center for Drug Screening, China Pharmaceutical University, 24 Tongjiaxiang, Nanjing 210009, PR China.*
[b]*Istituto di Cristallografia, Consiglio Nazionale delle Ricerche, Area Science Park-Basovizza, S.S. n° 14 Km 163.5, I-34149 Trieste, Italy.*
[c]*Department of Natural Medicinal Chemistry,* [d] *Department of Medicinal Chemistry, China Pharmaceutical University, 24 Tongjiaxiang, Nanjing 210009, PR China.*
[e]*Department for Life Quality Studies, University of Bologna, Corso d'Augusto 237, I-47921 Rimini*
[f]*Dipartimento di Scienze Chimiche e Farmaceutiche, Università di Trieste, Via L. Giorgieri 1, I-34127 Trieste, Italy.*
[g]*Institute of Biochemistry, Medical Faculty, University of Ljubljana, Vrazov trg 2, SI-1000 Ljubljana, Slovenia.*
[h]*Instituto Teófilo Hernando, Department of Pharmacology, Universidad Autónoma de Madrid, C/Arzobispo Morcillo 4, 28029 Madrid, Spain.*
[i]*Department of Pharmacy and Biotechnology, University of Bologna, via Belmeloro 6, I-40126 Bologna, Italy.*

Table of contents

SYNTHETIC PROCEDURES FOR INTERMEDIATES 4f AND 7.

11-Chloro-7,8,9,10-tetrahydro-6*H*-cyclohepta[*b*]quinoline (**7**). To a mixture of anthranilic acid (5.55 g, 40.5 mmol) and 1.1 molar equiv of cycloheptanone $POCl_3$ (33.6 mL) was added dropwise in ice bath. The reaction mixture was refluxed for 3h and cooled to r.t. and evaporated under reduced pressure. The residue was dissolved in 100 mL of CH_2Cl_2-CH_3OH (*v:v*, 2:1) and neutralized with a saturated K_2CO_3 solution and then washed with a saturated aqueous solution of sodium chloride (100 mL × 5). The organic layer was dried (Na_2SO_4) and evaporated under *vacuum* and purified by column chromatography (petroleum:EtOAc = 20:4, *v:v*) to afford **7**. Yield 80%. m.p. 89-91°C. ^{1}H NMR ($CDCl_3$, 300 MHz): δ ppm 8.19 (d, 1H, J = 8.1 Hz), 8.02 (d, 1H, J = 8.0 Hz), 7.78 (t, 1H, J = 7. 7 Hz), 7.57 (t, 1H, J = 8.0 Hz), 3.28-3.21 (m, 4H), 1.91-1.74 (m, 6H); MS (*m/z*): 232 ($[M+H]^+$).

N-(7,8,9,10-Tetrahydro-6*H*-cyclohepta[*b*]quinolin-11-yl)heptane-1,7-diamine (**4f**). 5 molar equiv of 1,7-diaminoheptane were added to 10 mL of 11-chloro-7,8,9,10-tetrahydro-6*H*-cyclohepta[*b*]quinoline (**7**) in pentanol. After refluxing for 30 h under nitrogen, the mixture was cooled to 0 °C and then acidified to pH = 2 with HCl/ether solution. The deposit was separated, dissolved in 10 mL of water, and then the solution was basified to pH = 10 with a saturated aqueous solution of Na_2CO_3 and extracted with CH_2Cl_2 (10 mL × 3). The organic layer were washed with a saturated aqueous solution of sodium chloride, dried over anhydrous Na_2SO_4, and evaporated *under vacuum*. The residue was purified by column chromatography (CH_2Cl_2:MeOH = 20:1.5, *v:v*, plus 0.5% triethylamine). Brown oil, yield 72%. ^{1}H NMR ($CDCl_3$, 300 MHz): δ ppm 8.01 (d, 1H, J = 8.3Hz), 7.92 (d, 1H, J = 8.3 Hz), 7.69 (t, 1H, J = 7.0 Hz), 3.34-3.29 (m, 2H), 3.22-3.20 (m, 2H), 2.94-2.90 (m, 2H), 2.88-2.86 (m, 2H), 2.04-1.84 (m, 10H), 1.52-1.40 (m, 6H). MS (*m/z*): 326 $[M+H]^+$.

Human AChE (*h*AChE) and BChE from human serum (*h*BChE) Inhibition Assay. AChE inhibitory activity was evaluated spectrophotometrically at 37 ºC by Ellman's method[1] using a Jasco V-530 double beam spectrophotometer. The rate of increase in the absorbance at 412 nm was followed for 5 min. AChE stock solution was prepared by dissolving recombinant *h*AChE (E.C.3.1.1.7) lyophilized powder (Sigma, Italy) in 0.1 M phosphate buffer (pH = 8.0) containing Triton X-100 0.1%. Stock solution of BChE (E.C. 3.1.1.8) from human serum (Sigma, Italy) was prepared by dissolving the lyophilized powder in an aqueous solution of gelatine 0.1%. Stock solutions of inhibitors (1 or 2 mM) were prepared in methanol. The assay solution consisted of a 0.1 M phosphate buffer pH 8.0, with the addition of 340 μM 5,5'-dithiobis(2-nitrobenzoic acid), 0.02 unit/mL *h*AChE or *h*BChE (Sigma Chemical), and 550 μM substrate (acetylthiocholine iodide or butyrylthiocholine iodide, respectively). 50 μL aliquots of increasing concentration of the tested compound were added to the assay solution and preincubated for 20 min at 37 °C with the enzyme followed by the addition of the substrate. Assays were carried out with a blank containing all components except *h*AChE or *h*BChE in order to account for the non-enzymatic reaction. The reaction rates were compared and the percent inhibition due to the presence of tested inhibitor at increasing concentration was calculated. Each concentration was analyzed in duplicate, and IC_{50} values were determined graphically from log concentration–inhibition curves (GraphPad Prism 4.03 software, GraphPad Software Inc.).

Kinetic analysis of *h*AChE inhibition. To gain insights into the mechanism of action of **2e**, reciprocal plots of 1/velocity *versus* 1/[substrate] were constructed at relatively low concentration of the substrate (0.56–0.11 mM) by using Ellman's method[1] and recombinant *h*AChE (Sigma, Milan, Italy). Three concentrations of **2e** were selected for this study: 0.20, 0.47, and 0.76 nM. The plots were assessed by a weighted least-squares analysis that assumed the variance of the velocity (v) to be a constant percentage of v for the entire data set. Calculation of the inhibitor constant (K_i) value

was carried out by re-plotting slopes of lines from the Lineweaver-Burk plot *versus* the inhibitor concentration and K_i was determined as the intersect on the negative x-axis. K'_i (dissociation constant for the enzyme–substrate–inhibitor complex) value was determined by plotting the apparent $1/v_{max}$ *versus* inhibitor concentration.[2] Data analysis was performed with GraphPad Prism 4.03 software (GraphPad Software Inc.).

Torpedo californica AChE inhibition by compound 2e

To determine the mode of action of *Torpedo californica* AChE (*Tc*AChE) inhibition by compound **2e**, we followed the time course of product formation on a BioLogic SFM2000 stopped flow apparatus at 25°C. The two phosphate buffer solutions (pH=7.0) were prepared as one containing the substrate ATCh, the Ellman's reagent (DTNB) and the tested compound, and the other that contained the *Tc*AChE. The buffer solutions were injected into a mixing chamber using syringes. The resulting solution, contained 80 µM ATCh, 1mM DTNB, 3.4 nM of *Tc*AChE and 1 to 10 nM of compound **2e**. The absorbance was followed at 412 nm immediately and until the change reached zero. The obtained progress curves were analyzed simultaneously with the ENZO package,[3] which can derives and numerically solve a system of differential equations and fits their coefficients. Several reaction mechanisms were tested. The simplest one for the reproduction of the progress curves in the absence or in the presence of compound **2e** was chosen, and the corresponding inhibition constants were determined.

The results file can be accessed by loading the ENZO project ID 140715968, selecting the "Set Parameters" tab, and pressing "Start''.

(http://enzo.cmm.ki.si/kinetic.php?uwd=140715968&load=true)

Potentiometric titration of compound 2e by *Tc*AChE

To diagnose the tight-binding of compound **2e** to *Tc*AChE, different concentrations of *Tc*AChE (0.1 – 2.0 nM) were incubated in phosphate buffer (pH=7.0) for 90 min with 0.3 nM of compound **2e**.

The residual *Tc*AChE activity was measured on a conventional spectrophotometer. The measurement was started by the addition of 4 μL of substrate (ATCh) solution into a final volume of 600 μL. The final ATCh concentration was 0.5 mM.

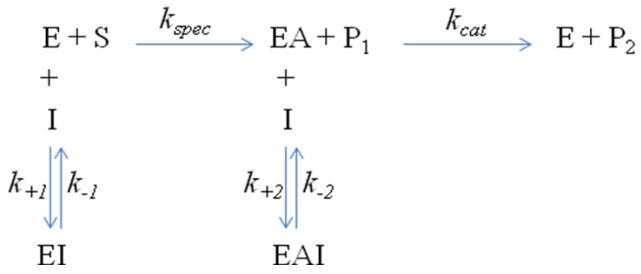

Scheme 2. Reaction Scheme of ATCh hydrolysis in the absence and presence of compounds **2e** (as well as **1e**, **1f**, **1h** and **3c**), as constructed by ENZO Web Tool (project no. 140715968)

E, EA, EI and EAI are free enzyme, acetylated enzyme, enzyme*inhibitor and acetylated enzyme-inhibitor complexes, respectively; S is the substrate (ATCh) , P_1 is choline and P_2 is acetate. k_{spec} is the second order specificity constant, k_{cat} is the catalytic constant, k_{+1}, k_{+2} are the second order association constants (k_{on}'s) and k_{-1}, k_{-2} the dissociation rate constants (k_{off}'s). Note that K_m is defined as k_{cat}/k_{spec}.

***h*AChE-induced Aβ$_{1–40}$ aggregation inhibition assay**.[4] Thioflavin T (Basic Yellow 1), recombinant *h*AChE lyophilized powder, 1,1,1,3,3,3-hexafluoro-2-propanol (HFIP), were purchased from Sigma Chemicals. Buffers and other chemicals were of analytical grade. Absolute DMSO over molecular sieves was from Fluka. Water was deionized and doubly distilled. Aβ$_{1–40}$, supplied as trifluoroacetate salt, was purchased from Bachem AG (Bubendorf, Switzerland). Aβ$_{1–40}$ (2 mg mL^{-1}) was dissolved in HFIP and lyophilized. The 1 mM solutions of tested inhibitors were prepared by dissolution in MeOH.

Aliquots of 2 μL Aβ$_{1–40}$ peptide, lyophilized from 2 mg mL^{-1} HFIP solution and dissolved in

DMSO, were incubated for 24 h at r.t. in 0.215 M sodium phosphate buffer (pH 8.0) at a final concentration of 230 μM. For co-incubation experiments aliquots (16 μL) of *h*AChE (final concentration 2.30 μM, Aβ/*h*AChE molar ratio 100:1) and *h*AChE in the presence of 2 μL of the tested inhibitor (final inhibitor concentration 100 μM) in 0.215 M sodium phosphate buffer pH 8.0 solution were added. Blanks containing $A\beta_{1\text{-}40}$ alone, recombinant *h*AChE alone, and $A\beta_{1–40}$ plus tested inhibitors in 0.215 M sodium phosphate buffer (pH 8.0) were prepared. The final volume of each vial was 20 μL. Each assay was run in duplicate. To quantify amyloid fibril formation, the thioflavin T fluorescence method was then applied.[5] The fluorescence intensities due to *β*-sheet conformation were monitored for 300 s at λ_{em} = 490 nm (λ_{exc} = 446 nm). The percent inhibition of the AChE-induced aggregation due to the presence of the tested compound was calculated by the following expression: $100 - (IF_i/IF_o \times 100)$ where IF_i and IF_o are the fluorescence intensities obtained for Aβ plus AChE in the presence and in the absence of inhibitor, respectively, minus the fluorescence intensities due to the respective blanks.

Inhibition of $A\beta_{1–42}$ self-aggregation. As reported in a previously published protocol,[6] HFIP pretreated $A\beta_{1–42}$ samples (Bachem AG, Switzerland) were solubilized with a CH_3CN/0.3 mM Na_2CO_3/250 mM NaOH (48.4:48.4:3.2) mixture. Experiments were performed by incubating the peptide in 10 mM phosphate buffer (pH = 8.0) containing 10 mM NaCl, at 30 °C for 24 h (final Aβ concentration = 50 μM) with and without inhibitor (10 μM, Aβ/inhibitor = 5/1). Blanks containing the tested inhibitors were also prepared and tested. To quantify amyloid fibrils formation, the thioflavin T fluorescence method was used.[5] After incubation, samples were diluted to a final volume of 2.0 mL with 50 mM glycine–NaOH buffer (pH 8.5) containing 1.5 μM thioflavin T. A 300 s-time scan of fluorescence intensity was carried out (λ_{exc} = 446 nm; λ_{em} = 490 nm, FP-6200 fluorometer, Jasco Europe), and values at plateau were averaged after subtracting the background fluorescence of 1.5 μM thioflavin T solution. The fluorescence intensities were compared and the

percent inhibition due to the presence of the inhibitor was calculated by the following formula: 100 − ($IF_i/IF_o \times 100$) where IF_i and IF_o are the fluorescence intensities obtained for $A\beta_{1-42}$ in the presence and in the absence of inhibitor, respectively.

BACE-1 Inhibition Assay. Inhibition studies on recombinant human BACE-1 (*h*BACE-1, Sigma, Italy) were performed by employing a peptide mimicking APP sequence as substrate (Methoxycoumarin-Ser-Glu-Val-Asn-Leu-Asp-Ala-Glu-Phe-Lys-dinitrophenyl, M-2420, Bachem, Germany). The following procedure was employed: 5 μL of test compounds (or DMSO, if preparing a control well) were pre-incubated with 175 μL of enzyme (in 20 mM sodium acetate containing CHAPS 0.1% w/v) for 1 h at r.t. The substrate (3 μM, final concentration) was then added and left to react for 15 min at 37°C. The fluorescence signal was read at λ_{em} = 405 nm (λ_{exc} = 320 nm) using a Fluoroskan Ascent. The DMSO concentration in the final mixture maintained below 5% (*v/v*) guaranteed no significant loss of enzyme activity. The fluorescence intensities with and without inhibitor were compared and the percent inhibition due to the presence of test compounds was calculated. The background signal was measured in control wells containing all the reagents, except *h*BACE-1 and subtracted. The % inhibition due to the presence of increasing test compound concentration was calculated by the following expression: 100-(IF_i/IF_o x 100) where IF_i and IF_o are the fluorescence intensities obtained for *h*BACE-1 in the presence and in the absence of inhibitor, respectively. Inhibition curves were obtained by plotting the % inhibition *versus* the logarithm of inhibitor concentration in the assay sample, when possible. The linear regression parameters were determined and the IC_{50} extrapolated (GraphPad Prism 4.0, GraphPad Software Inc.). To demonstrate inhibition of *h*BACE-1 activity a peptido-mimetic inhibitor (β-secretase inhibitor IV, Calbiochem) was serially diluted into the reactions' wells (IC_{50} = 20 nM).

Cell culture of the human neuroblastoma cell line SH-SY5Y

Cell culture of the human neuroblastoma cell line SH-SY5Y. SH-SY5Y cells were maintained in a

1:1 mixture of F-12 nutrient mixture (Ham12) (Sigma–Aldrich, Spain) and Eagle's minimum essential medium (EMEM) supplemented with 15 nonessential amino acids, 1 mM sodium pyruvate, 10% heat-inactivated foetal bovine serum (FBS), 100 U/mL penicillin, and 100 μg/mL streptomycin (reagents from Invitrogen, Spain). Cultures were seeded into flasks containing supplemented medium and maintained at 37 °C in a humidified atmosphere of 5% CO_2 and 95% air. For assays, SH-SY5Y cells were sub-cultured in 48-well plates at a seeding density of 1 × 105 cells per well. Cells were treated with the tested compound before confluence in F12/EMEM with 1% FBS. All the cells used in this study were used at a low passage number (<13).

To evaluate the effects of selected hybrids and tacrine on cell viability, SH-SY5Y cells were incubated for 48 h with 3, 10, 30 μM of , and thereafter, cell viability was measured as MTT reduction.

Measurement of cell viability with MTT. Cell viability, virtually the mitochondrial activity of living cells, was measured by quantitative colorimetric assay with MTT (3-[4,5-dimethylthiazol-2-yl]-2,5-diphenyltetrazolium bromide, Sigma–Aldrich, Spain), as described previously.[7] MTT was added to all wells (final concentration 0.5 mg/mL) and allowed to incubate in the dark at 37 °C for 2 h. The tetrazolium ring of MTT can be cleaved by mitochondrial reductases in order to produce a precipitated formazan derivative. After this 2 h period, the formazan produced was dissolved by adding 200 μL of DMSO, resulting in a colored compound whose optical density was measured in an ELISA reader at 540 nm. All MTT assays were performed in triplicate. Absorbance values obtained in control cells untreated with the toxic were considered as 100% viability.

Table S1. Summary of Crystallographic Data of the *Tc*AChE-**2e** complex

Data Collection	
X-ray source	XRD-1 ELETTRA, Trieste (Italy)
Wavelength (Å)	1.00
Detector	Pilatus 2M – Dectris Ltd.
Space group	$P3_121$
Unit cell parameters	
a,b (Å)	112.22
c (Å)	138.72
Mosaicity (°)	0.75
Resolution range (Å)	46.22−2.80 (2.80−2.95)[a]
Number of measurements	113892
Number of unique reflections ($I \geq 0$)	22808 (3319)
Completeness (%)	90.0 (90.8)
multiplicity	5.0 (5.1)
$\langle I/\sigma(I)\rangle$	11.7 (3.4)
R_{merge}[b]	0.090 (0.386)
R_{pim}[b]	0.040 (0.171)
R_{meas}[b]	0.099 (0.426)
$CC_{1/2}$	0.996 (0.937)
CC*	0.999 (0.967)
Refinement Statistics	
Resolution range (Å)	45.90−2.80
Number of reflections ($F_o \geq 0$)	21631
R_{work}[c]	0.192
R_{free}[d]	0.260
Number of atoms	
Non-hydrogen protein	4263
Non-hydrogen waters	95
Non-hydrogen inhibitor (**2**$_5$)	33
Non-hydrogen carbohydrates	56
Rmsd bond lengths/bond angles (Å, deg)[e]	0.013/1.8
Ramachandran plot (%) favored/allowed regions (%)[f]	90.40/99.20
Average Temperature Factors (Å^2)	
Protein	60.3
Water	53.8
Inhibitor	48.6
Carbohydrates	89.2
Rmsd ΔB (Å^2)[g]	4.79

[a]Number in parentheses refer to the highest resolution shell.

[b]$R_{merge} = \sum_{\mathbf{h}}\sum_i \left| I_{\mathbf{h}i} - \langle I_{\mathbf{h}}\rangle \right| / \sum_{\mathbf{h}}\sum_i I_{\mathbf{h}i}$, with $I_{\mathbf{h}}$ is the ith measurement of reflection **h**, and $\langle I_{\mathbf{h}}\rangle$ is the (weighted) average of all symmetry-related or replicate observations of the unique reflection **h**. The summations include all "n" observed reflections; $R_{pim} = \sum_{\mathbf{h}} (1/n\text{-}1)^{1/2} \sum_i \left| I_{\mathbf{h}i} - \langle I_{\mathbf{h}}\rangle \right| / \sum_{\mathbf{h}}\sum_i I_{\mathbf{h}i}$; $R_{meas} = \sum_{\mathbf{h}} (n/n\text{-}1)^{1/2} \sum_i \left| I_{\mathbf{h}i} - \langle I_{\mathbf{h}}\rangle \right| / \sum_{\mathbf{h}}\sum_i I_{\mathbf{h}i}$

[c]$R_{work} = \sum_{\mathbf{h}} \left| F_o \right| - \left| F_c \right| / \sum_{\mathbf{h}} \left| F_o \right|$, where $\left| F_o \right|$ and $\left| F_c \right|$ are the observed and calculated structure factor amplitudes for reflection h. The summation is extended over all unique reflections to the specified resolution.

[d]R_{free}, R factor calculated using 1132 randomly chosen reflections (5%) set aside from all stages of refinement.

[e]Stereochemical criteria are those of Engh and Huber.[8]

[f]The reliability of the protein structure has been assessed using the MolProbity package.[9]
There are four outliers: Phe284, Asp285, Asp380 and His 486.

[g]Rmsd ΔB is the rms deviation of the B factor of bonded atoms.[10]

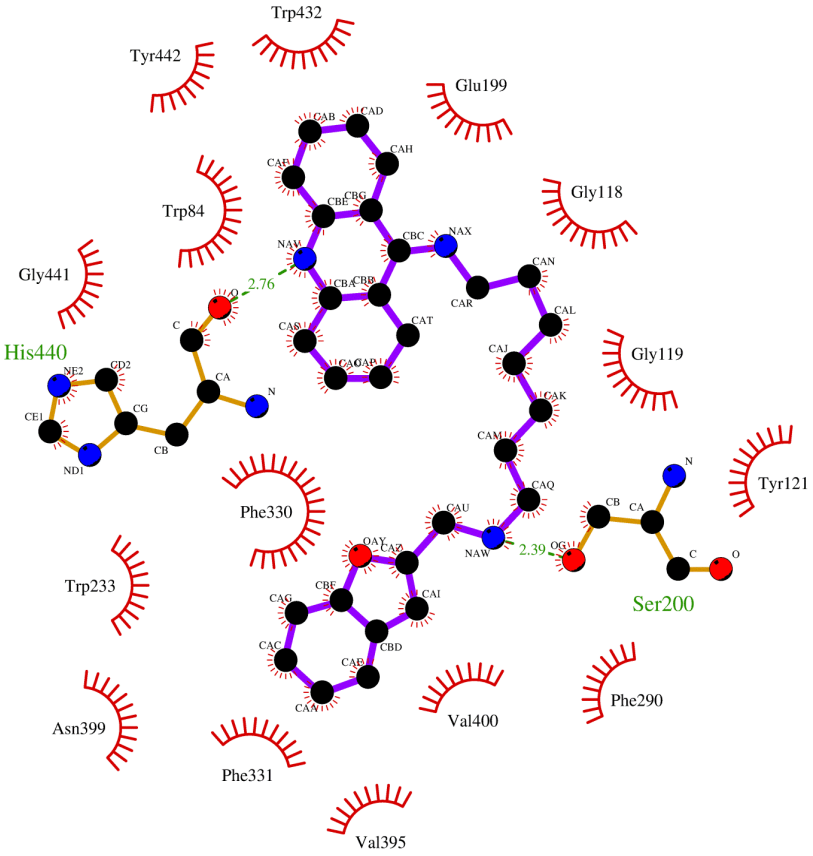

Figure S1. Ligplot+[11] representation of the interactions of **2e** with *Tc*AChE. Hydrogen bonding interactions are drawn as dashed lines.

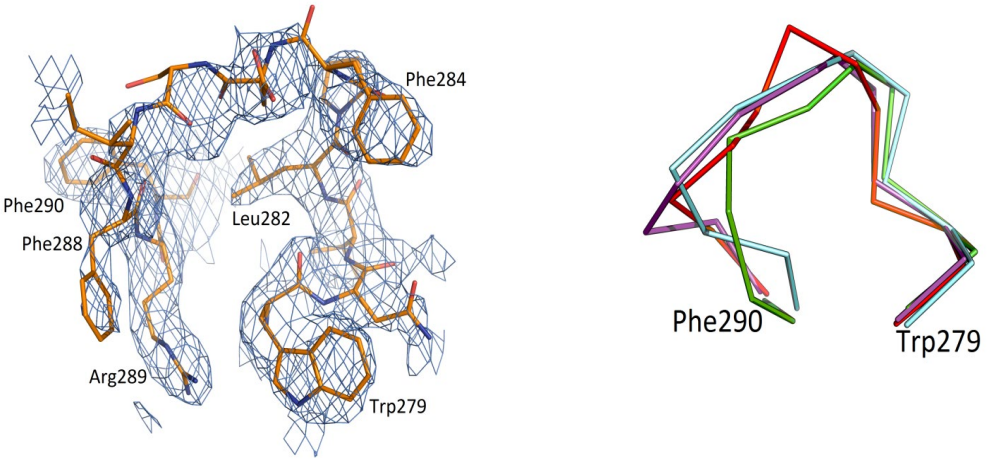

A **B**

Figure S2. (A**)** The final $2F_o - F_c$ σA-weighted electron density map for residues Trp279-Phe290. Contouring is at 1.0 σ, at a radius of 2.5 Å from each atom in the loop. The protein is rendered as a stick model with carbon, oxygen, and nitrogen atoms colored orange, red, and blue, respectively
(B) Comparison of the conformational plasticity of the Trp279-Phe290 segment (C_α trace) in the apo *Tc*AChE[5] (magenta), *Tc*AChE-bis(5)tacrine[6] (red), the aged phosphonylated *Tc*AChE[7] (cyan) and *Tc*AChE-**2e** (green) structures. The figures were created using PyMOL (http://www.pymol.org).

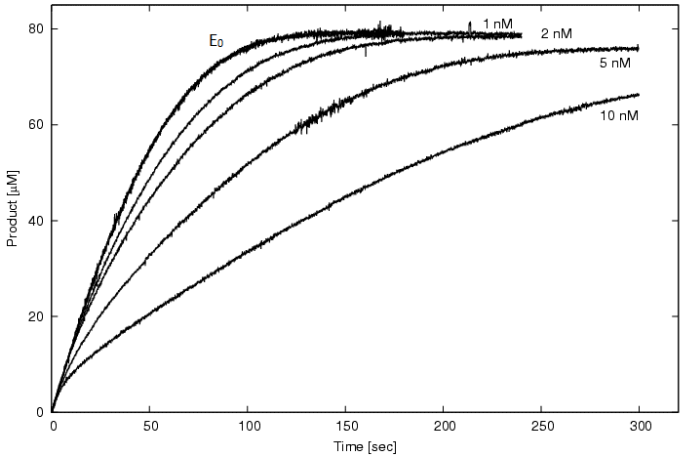

Figure S3. Progress curves for hydrolysis of ATCh by *Tc*AChE in the absence (E_0) and in the presence of compound **2e** (1, 2, 5 and 10 nM) measured on a BioLogic SFM2000 stopped flow apparatus. The initial *Tc*AChE and ATCh concentrations were 3.4 nM and 80 μM respectively.

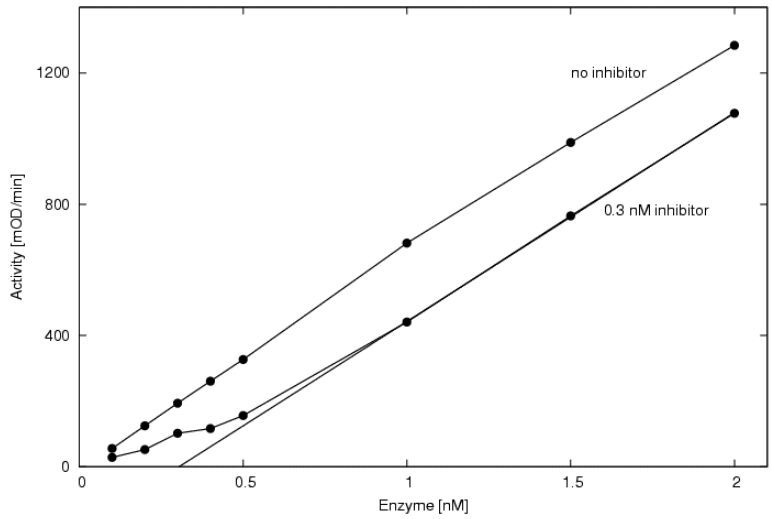

Figure S4. Potentiometric titration of compound **2e** (0.3 nM) by different concentrations of *Tc*AChE (0.1-2.0 nM). The enzyme and the inhibitor were pre-incubated 90 min prior to the addition of 0.5 mM ATCh (final concentration).

***Tc*AChE inhibition by compounds 1e, 1f, 1h and 3c.**

The measurements with compounds **1e, 1f, 1h** and **3c** were carried out on a conventional spectrophotometer (Perkin-Elmer LS40) under essentially the same conditions as for those performed on the stopped flow apparatus. The concentrations of the reactants, however, were adjusted in order to explore the reaction over a long period of time. Consequently, the concentrations of each individual inhibitor (5 – 20 nM) were at least five times higher than the *Tc*AChE concentration (0.5 - 1 nM) used. In this conditions, the observed kink in the initial portion of the progress curves became insignificant. The analysis was perform by assuming the same kinetic model employed for the analysis of the progress curves in the presence of compound **2e**.

Kinetic evaluation of compounds 1e, 1f, 1h and 3c on *Tc*AChE

The inhibition of *Tc*AChE by **1e, 1f, 1h** and **3c** was measured following the time course of the reaction on a conventional spectrophotometer. Since the enzyme concentrations were at least five times lower than of the lowest inhibitor concentration being used, the kink were observed in the very beginning of the curve reactions, just at the dead time of the conventional kinetic measurements, became insignificant. However, the analysis of the progress curves by exploiting the same reaction model used for compound **2e**, resulted in comparable high affinity inhibition constants (see **Table S2**).

Table S2. Characteristic constants for the hydrolysis of ATCh by *Tc*AChE and its inhibition by compounds **2e, 1e, 1f, 1h** and **3c** at pH=7.0.

			Competitive	**Non-competitive**
K_m (μM)		54.6 ± 0.5		
k_{cat} (s^{-1})		688 ± 4		
k_{on} (M^{-1} s^{-1})	**2e**		1.45 ± 0.7 x 10^7	1.45 x 10^7
k_{off} (s^{-1})	**2e**		0.032 ± 0.0002	0.031 ± 0.0004
K_i (nM)	**2e**		2.2	2.1
k_{on} (M^{-1} s^{-1})	**1e**		1.6 ± 0.2 x 10^6	1.3 ± 0.1 x 10^7
k_{off} (s^{-1})	**1e**		0.006 ± 0.0005	0.029 ±- 0.003
K_i (nM)	**1e**		3.8	2.3
k_{on} (M^{-1} s^{-1})	**1f**		4.9 ± 0.9 x 10^6	4.9 x 10^6
k_{off} (s^{-1})	**1f**		0.021 +/- 0.0004	0.021
K_i (nM)	**1f**		4.4	4.4
k_{on} (M^{-1} s^{-1})	**1h**		3.1 ± 0.7 x 10^7	3.1 x 10^7
k_{off} (s^{-1})	**1h**		0.011 ± 0.0002	0.011
K_i (nM)	**1h**		0.35	0.35
k_{on} (M^{-1} s^{-1})	**3c**		8.7 ± 0.5 x 10^6	8.7 x 10^6
k_{off} (s^{-1})	**3c**		0.044 ± 0.003	0.040 ± 0.003
K_i (nM)	**3c**		5.0	4.5

A

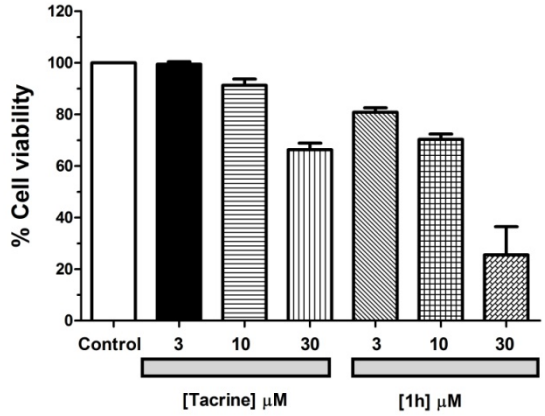

B

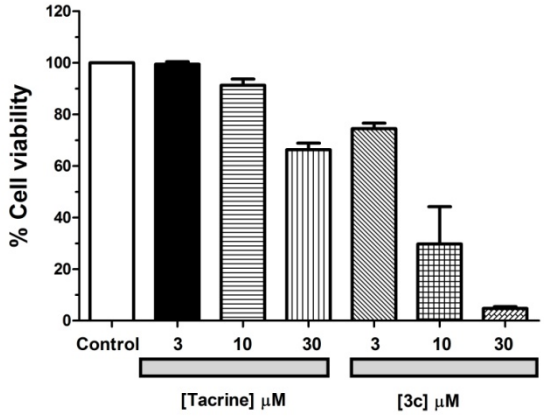

Figure S5. Cell viability, measured as reduction of MTT, in SH-SY5Y cells exposed for 48 h with increasing concentrations of (A) **1h** or (B) **3c** in comparison with tacrine. Data correspond to the mean and S.E.M. of 4 different experiments performed in triplicate.

Table S3. Effects of oral administration of **2e** (20 μmol/kg) and tacrine (20 μmol/kg) in the scopolamine-induced memory impairment evaluated by the Morris water maze test in mice. Data are presented as means ± SEM (n = 9-10, * *p<0.05, ** p<0.01, vs Sham group*, ## *p<0.01, vs Scop group*).

Group	Escape Latency (s)				
	day 1	day 2	day 3	day 4	day 5
Sham	37.3±5.6	21.4±3.2	37.9±8.9	28.5±6.0	21.1±4.6**
Scop[a]	43.9±6.6	30.5±5.7	51.6±6.6	44.5±8.2	45.7±6.3##
Tacrine + Scop	39.3±5.8	23.2±3.8	39.6±6.9	32.5±5.8	27.7±5.9*
2e + Scop	33. 8±6.6	19.2±3.1	43.1±7.9	30.1±5.3	25.1±5.6*

[a.] Scop stands for scopolamine.

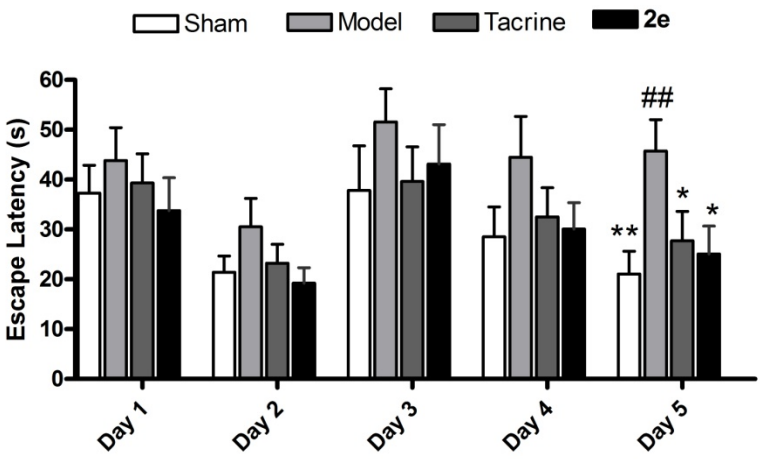

Figure S6. Total time left in the fourth quadrant. In the probe trial on day 6, administration of **2e** significantly improved overall target quadrant preference (36.25%, ** $p<0.01$) , in comparison to tacrine treated group (32.5%, *$p<0.05$). These results indicated that **2e** considerably ameliorated cognition impairment of treated mice.

Table S4. Effects of oral administration of **2e** and tacrine on spatial bias (% of total distance swum in the training quadrant during spatial probe trial). Data are presented as means ± S.E.M. (n = 9-10, * *p<0.05,* ** *p<0.01, vs Sham group*, ## *p<0.01, vs Scop group*).

Group	Percentage of path length in the target quadrant	Swimming time in the target quadrant (s)
Sham	41.3±5.0**	42.9±5.2**
Scop[a]	22.9±1.9##	21.2±2.1##
Tacrine + Scop[a]	32.5±4.1*	32.1±3.6*
2e + Scop [a]	36.3±3.6**	39.4±4.9**

[a] Scop stands for scopolamine.

Table S5. HPLC analysis data of compounds **1a-1l, 2a-2f, 3a-3h**. The purities of compounds were determined by the methods as shown given in the following table. The peak purity was checked with UV spectra.

Equipment		SHIMADZU LC2010 with binary pump equipped with a photodiode array detector (DAD)		
Column		SHIMADZU Shim-Pack VP-ODS (150×4.6 mm i.d., 5 μm particle size)		
Methods		a. CH_3OH/H_2O/TFA, 60/40/0.1 (v/v/v), flow rate: 1.0 mL /min, λ = 254 nm		
		b. CH_3OH/H_2O/TFA, 55/45/0.1 (v/v/v), flow rate: 1.0 mL /min, λ = 254 nm		
		c. CH_3OH/H_2O/TFA, 50/50/0.1 (v/v/v), flow rate: 1.0 mL /min, λ = 254 nm		
		d. CH_3OH/H_2O/TFA, 45/55/0.1 (v/v/v), flow rate: 1.0 mL /min, λ = 254 nm		
Results	Compd	Methods	Retention time (min)	Relative purity (%)
	1a	a	8.750	98.97
	1b	b	10.385	97.11
	1c	a	12.244	97.31
	1d	a	9.750	97.86
	1e	b	10.229	95.99
	1f	a	7.471	97.23
	1g	a	6.296	98.44
	1h	a	7.419	95.96
	1i	a	18.041	97.30
	1j	a	6.703	97.73
	1k	a	8.135	98.40
	1l	a	9.287	99.73
	2a	b	13.568	97.14
	2b	a	6.354	98.87
	2c	b	3.185	99.93
	2d	b	3.183	99.70
	2e	b	3.424	99.47
	2f	c	6.023	99.67
	3a	a	6.764	98.79
	3b	a	5.363	96.83
	3c	a	3.986	95.39
	3d	c	4.587	96.91
	3e	c	4.549	95.50
	3f	d	10.553	97.26
	3g	c	5.831	96.93
	3h	d	11.046	97.92

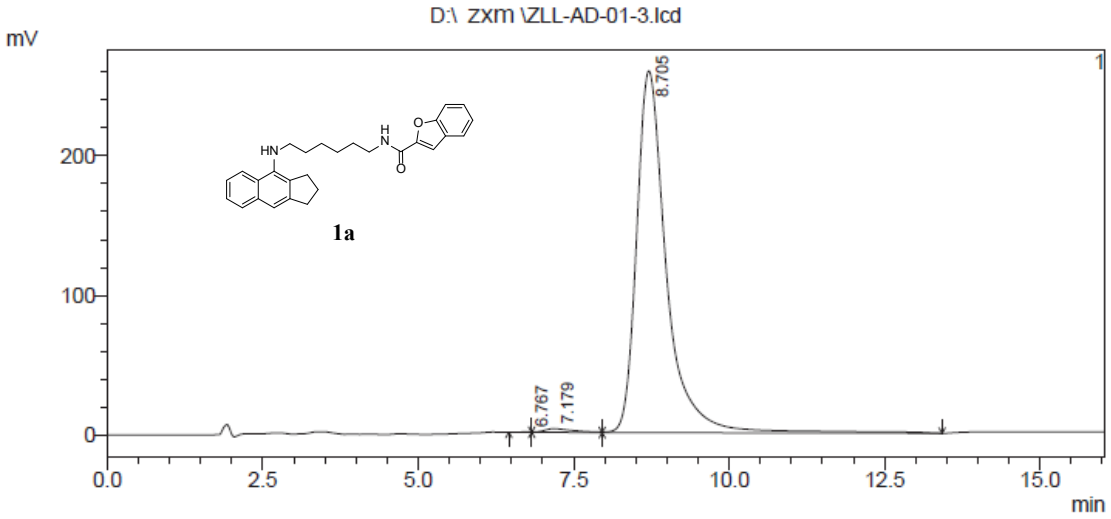

1a

Peak Table

Detector A Ch1 254nm

Peak#	R.T.	Area	Height	Area %	Height %
1	6.767	3240	246	0.037	0.094
2	7.179	87420	2720	0.992	1.038
3	8.705	8722252	259111	98.971	98.869
Total		8812912	262077	100.000	100.000

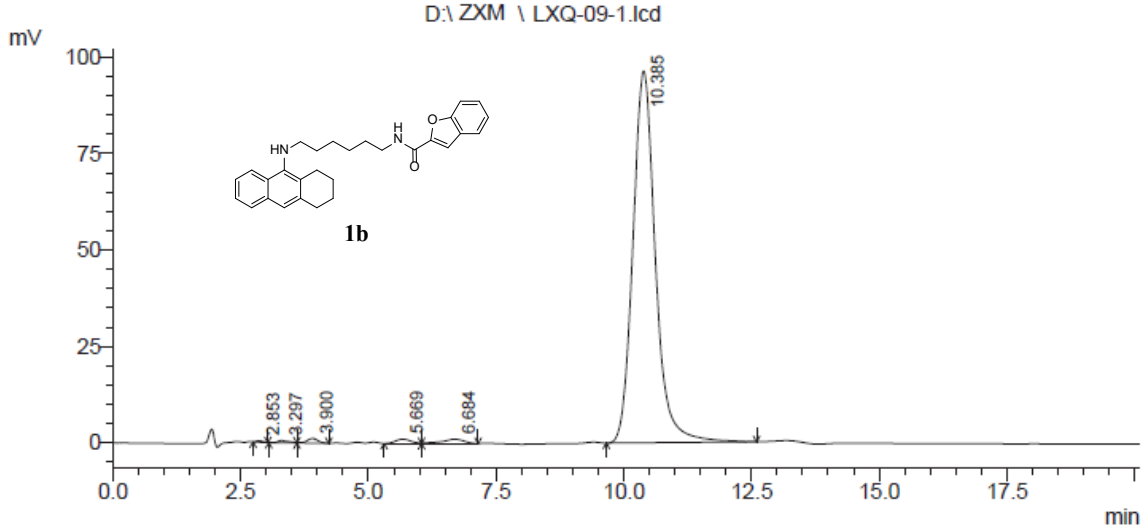

1b

Peak Table

Detector A Ch1 254nm

Peak#	R.T.	Area	Height	Area %	Height %
1	2.853	3238	373	0.107	0.370
2	3.297	8601	558	0.283	0.554
3	3.900	18703	1262	0.616	1.252
4	5.669	23703	1150	0.781	1.141
5	6.684	33395	1149	1.101	1.139
6	10.385	2946568	96327	97.112	95.544
Total		3034208	100819	100.000	100.000

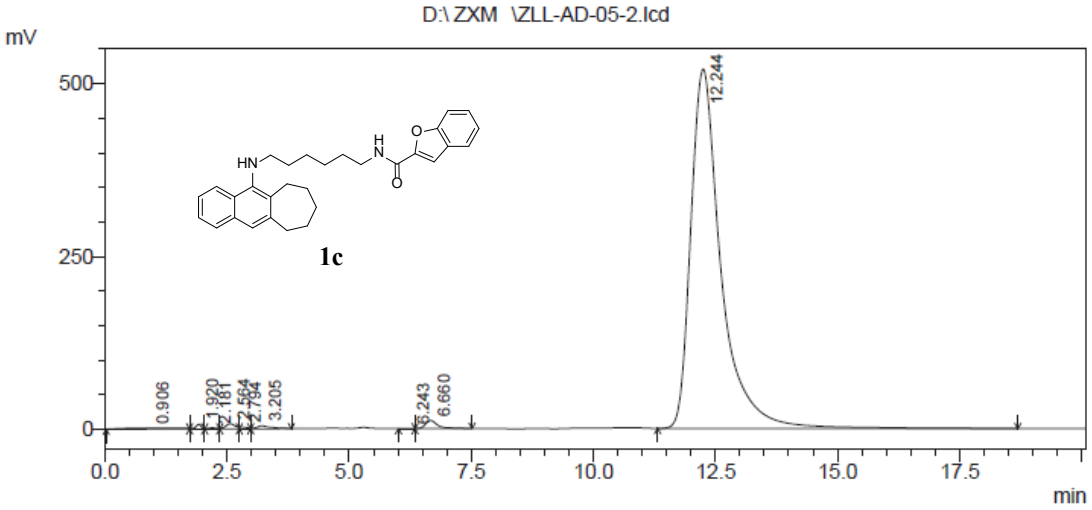

Peak Table

Detector A Ch1 254nm

Peak#	R.T.	Area	Height	Area %	Height %
1	0.906	128620	1581	0.558	0.284
2	1.920	52204	6737	0.226	1.212
3	2.181	21409	1521	0.093	0.274
4	2.564	100578	7128	0.436	1.282
5	2.794	25988	2497	0.113	0.449
6	3.205	87938	4467	0.381	0.804
7	6.243	2852	230	0.012	0.041
8	6.660	201979	11712	0.876	2.107
9	12.244	22438580	520002	97.305	93.546
Total		23060148	555877	100.000	100.000

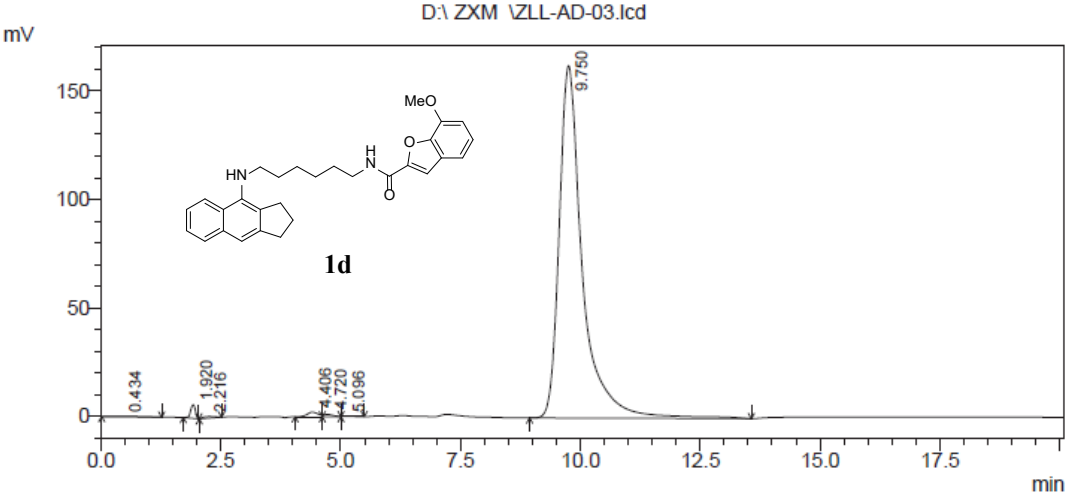

Peak Table

Detector A Ch1 254nm

Peak#	R.T.	Area	Height	Area %	Height %
1	0.434	10116	240	0.180	0.139
2	1.920	42524	6247	0.757	3.609
3	2.216	12656	762	0.225	0.440
4	4.406	35258	2153	0.628	1.244
5	4.720	16011	1115	0.285	0.644
6	5.096	3751	244	0.067	0.141
7	9.750	5494334	162319	97.857	93.783
Total		5614649	173080	100.000	100.000

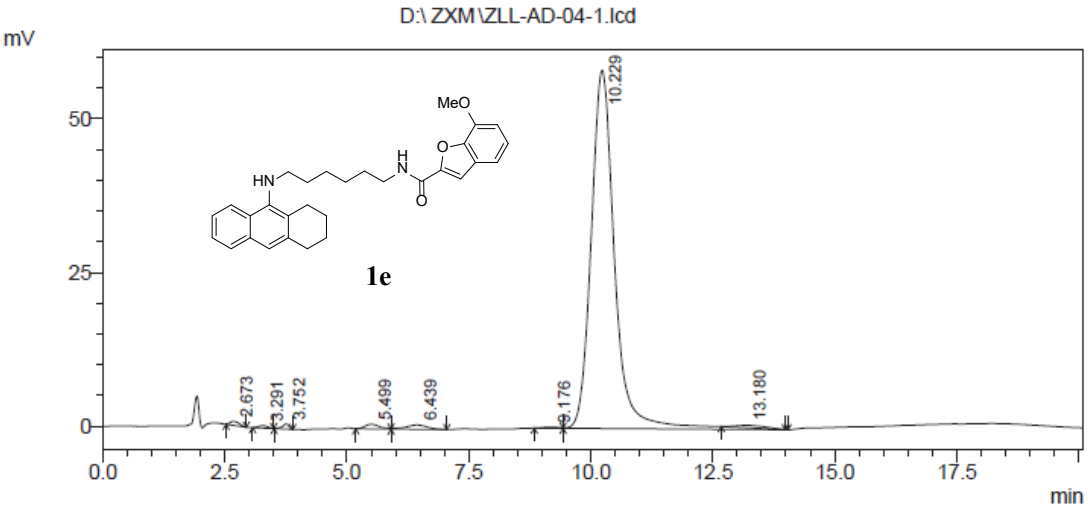

Peak Table

Detector A Ch1 254nm

Peak#	R. T.	Area	Height	Area %	Height %
1	2. 673	8384	658	0. 412	1. 058
2	3. 291	5228	403	0. 257	0. 648
3	3. 752	7743	842	0. 381	1. 353
4	5. 499	16071	768	0. 790	1. 233
5	6. 439	22221	715	1. 092	1. 149
6	9. 176	4303	203	0. 211	0. 326
7	10. 229	1953262	58272	95. 985	93. 604
8	13. 180	17759	392	0. 873	0. 630
Total		2034970	62254	100. 000	100. 000

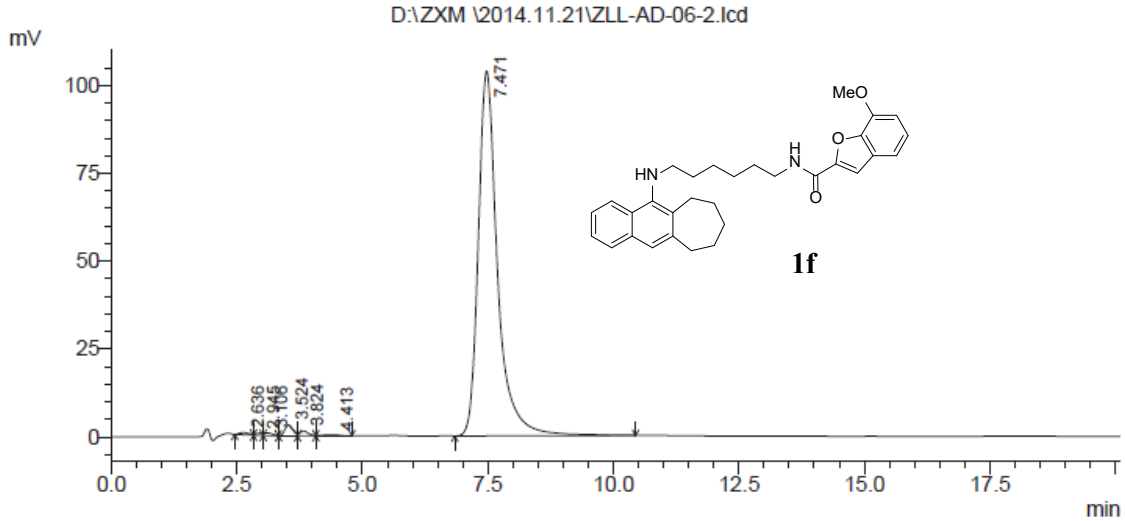

Peak Table

Detector A Ch1 254nm

Peak#	R. T.	Area	Height	Area %	Height %
1	2. 636	8431	629	0. 296	0. 569
2	2. 945	5284	606	0. 185	0. 548
3	3. 106	8153	754	0. 286	0. 681
4	3. 524	34556	3113	1. 212	2. 814
5	3. 824	16302	1415	0. 572	1. 279
6	4. 413	6351	279	0. 223	0. 252
7	7. 471	2772036	103826	97. 226	93. 856
Total		2851113	110622	100. 000	100. 000

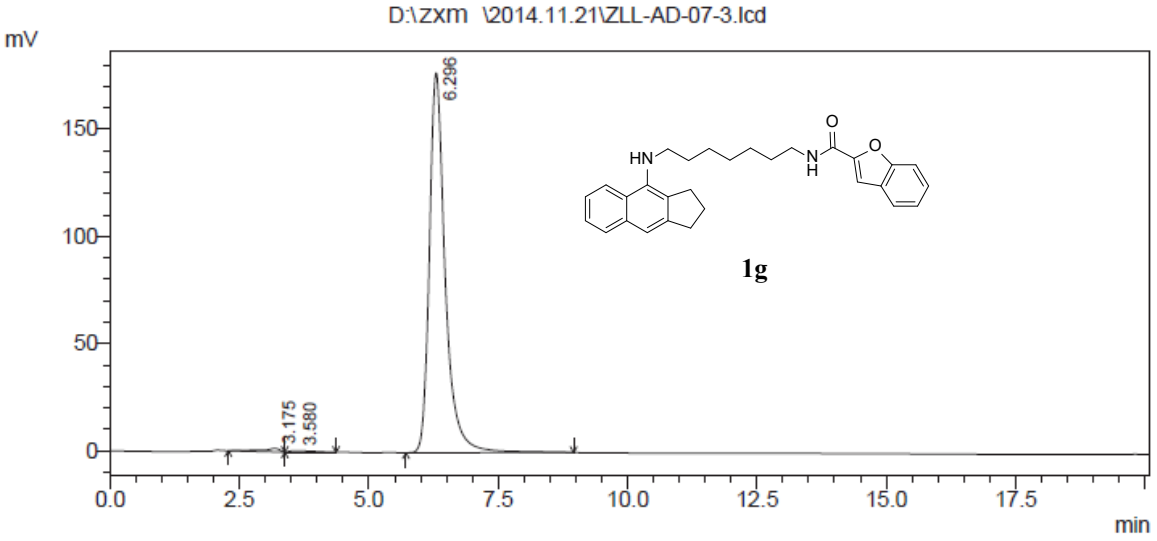

1g

Peak Table

Detector A Ch1 254nm

Peak#	R.T.	Area	Height	Area %	Height %
1	3.175	39857	1606	1.037	0.895
2	3.580	20225	636	0.526	0.354
3	6.296	3785046	177172	98.437	98.751
Total		3845129	179413	100.000	100.000

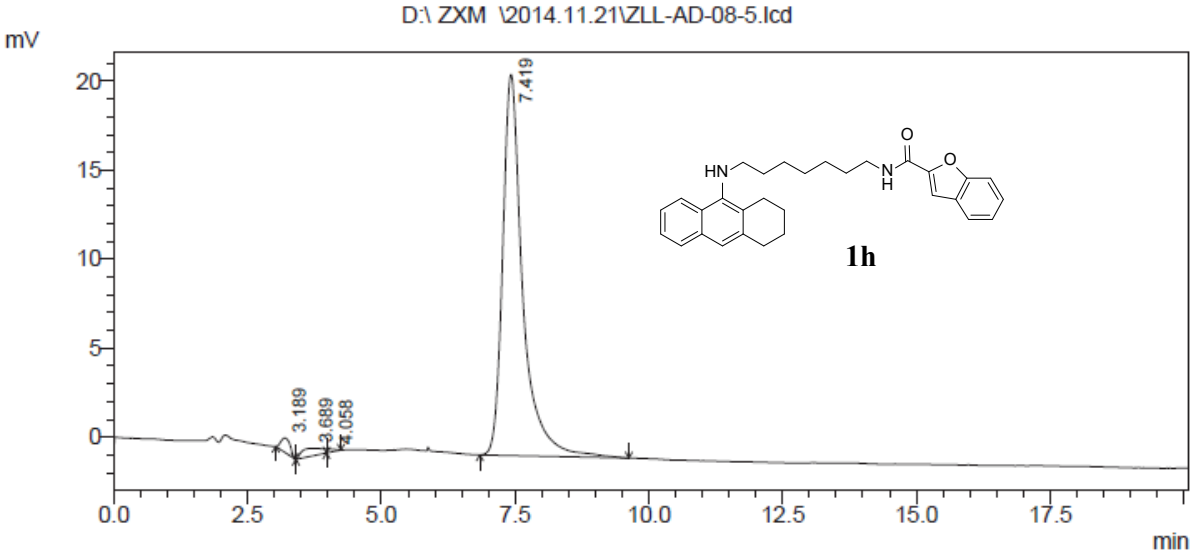

1h

Peak Table

Detector A Ch1 254nm

Peak#	R.T.	Area	Height	Area %	Height %
1	3.189	9831	811	1.689	3.552
2	3.689	11817	436	2.030	1.911
3	4.058	1882	169	0.323	0.740
4	7.419	558616	21408	95.958	93.796
Total		582147	22824	100.000	100.000

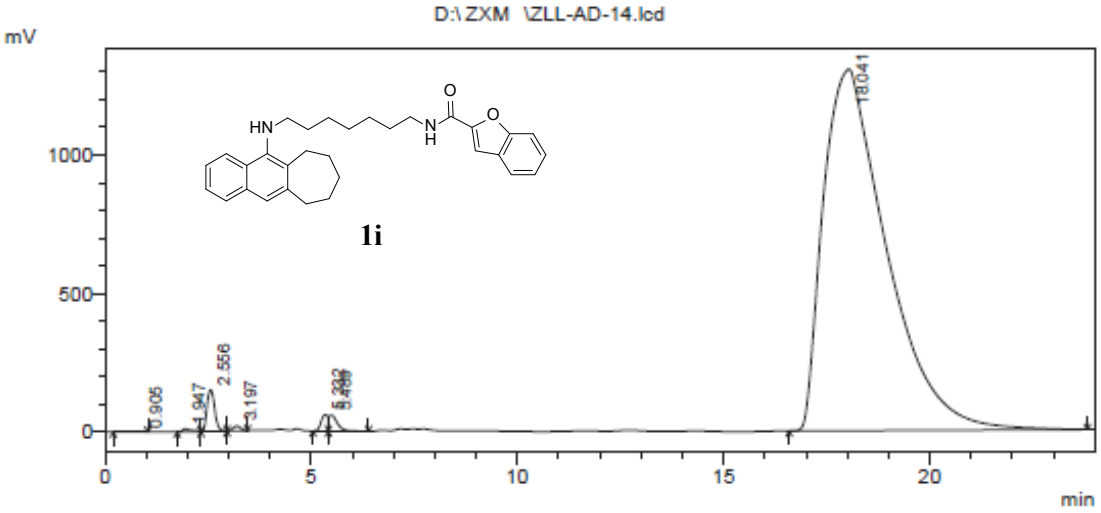

Peak Table

Detector A Ch1 254nm

Peak#	R.T.	Area	Height	Area %	Height %
1	0.905	1336	49	0.001	0.003
2	1.947	174355	11228	0.122	0.701
3	2.556	1954602	149939	1.368	9.364
4	3.197	234150	18855	0.164	1.178
5	5.332	669691	58765	0.469	3.670
6	5.489	824418	56934	0.577	3.556
7	18.041	139059645	1305384	97.300	81.528
Total		142918196	1601155	100.000	100.000

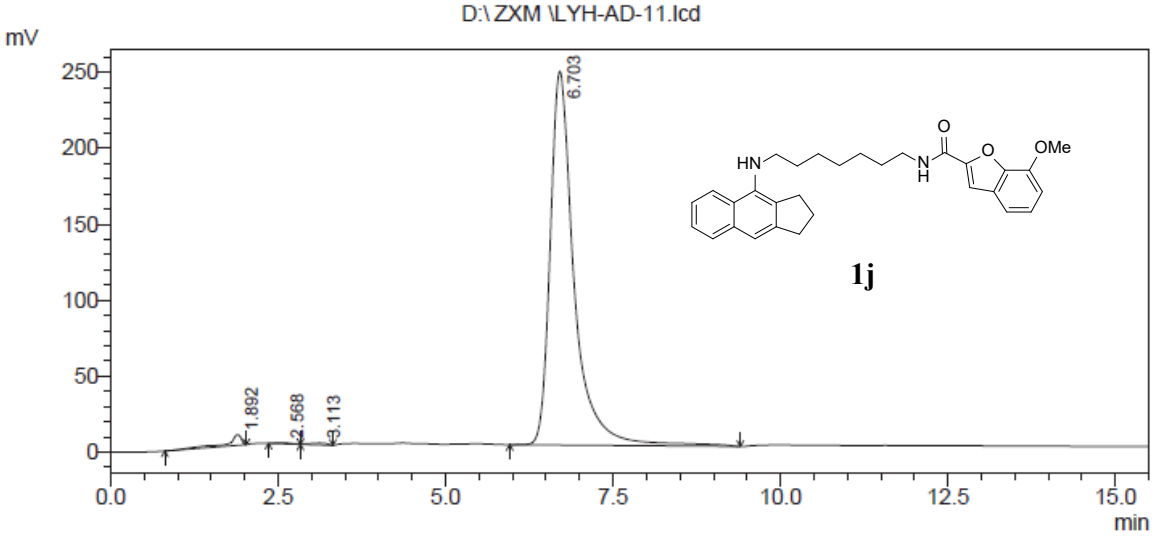

Peak Table

Detector A Ch1 254nm

Peak#	R.T.	Area	Height	Area %	Height %
1	1.892	105691	6998	1.678	2.741
2	2.568	13644	779	0.217	0.305
3	3.113	23945	1249	0.380	0.489
4	6.703	6154872	246271	97.725	96.465
Total		6298151	255296	100.000	100.000

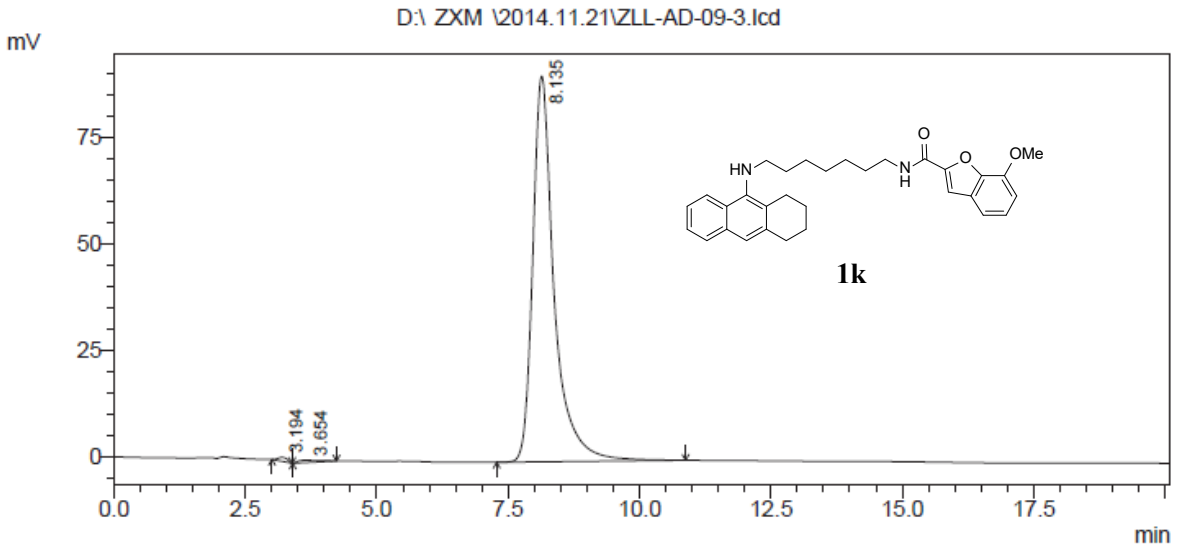

1k

Peak Table

Detector A Ch1 254nm

Peak#	R.T.	Area	Height	Area %	Height %
1	3.194	11662	926	0.450	1.008
2	3.654	15713	545	0.606	0.593
3	8.135	2565951	90407	98.944	98.399
Total		2593326	91878	100.000	100.000

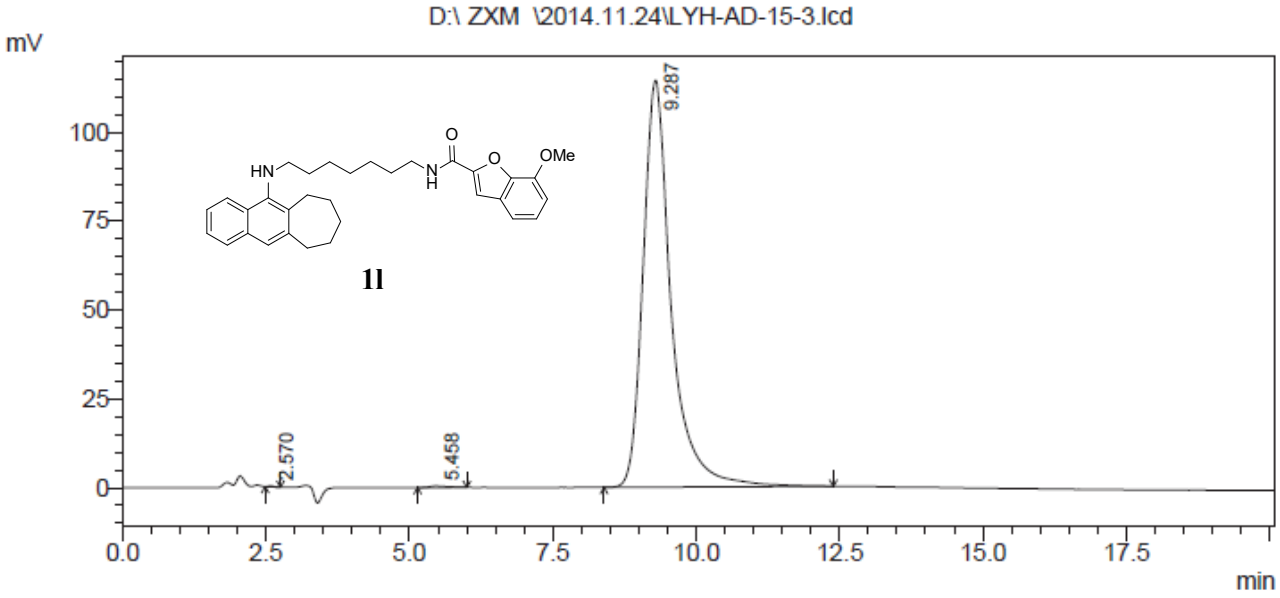

1l

Peak Table

Detector A Ch1 254nm

Peak#	R.T.	Area	Height	Area %	Height %
1	2.570	1937	294	0.049	0.255
2	5.458	8791	440	0.224	0.382
3	9.287	3912762	114492	99.727	99.363
Total		3923489	115227	100.000	100.000

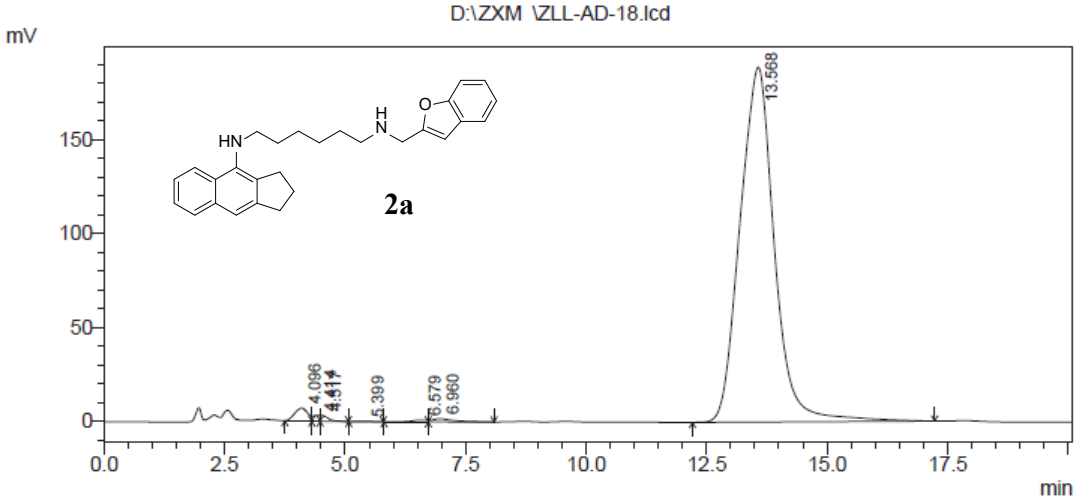

Peak Table

Detector A Ch1 254nm

Peak#	R.T.	Area	Height	Area %	Height %
1	4.096	128513	6872	1.335	3.355
2	4.414	31254	3142	0.325	1.534
3	4.517	34916	3108	0.363	1.517
4	5.399	4832	225	0.050	0.110
5	6.579	21461	884	0.223	0.432
6	6.960	54602	1779	0.567	0.868
7	13.568	9348751	188806	97.137	92.183
Total		9624329	204816	100.000	100.000

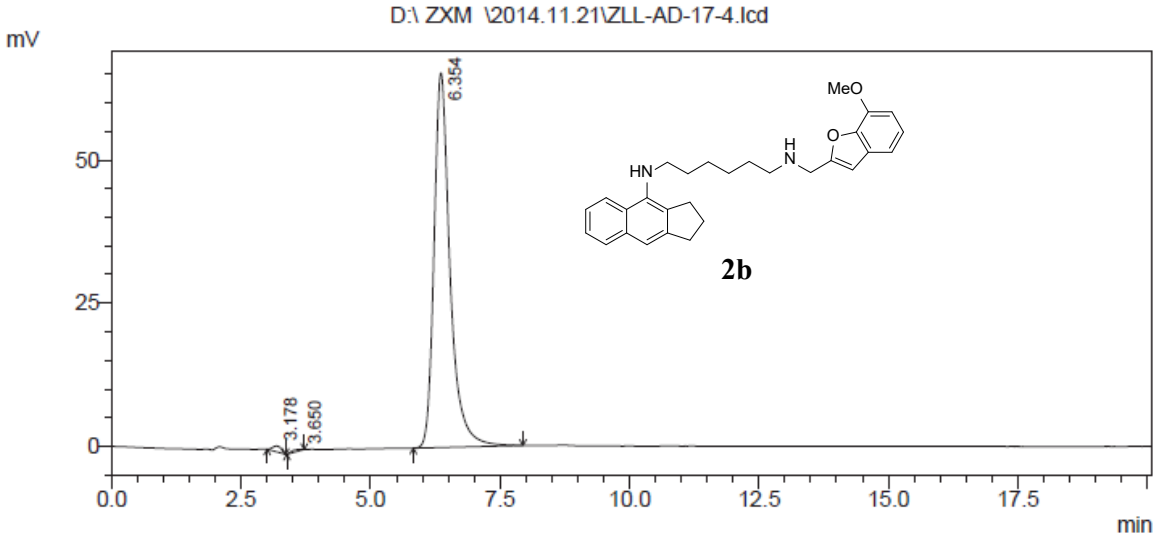

Peak Table

Detector A Ch1 254nm

Peak#	R.T.	Area	Height	Area %	Height %
1	3.178	11750	994	0.824	1.493
2	3.650	4409	163	0.309	0.245
3	6.354	1409782	65381	98.867	98.262
Total		1425941	66537	100.000	100.000

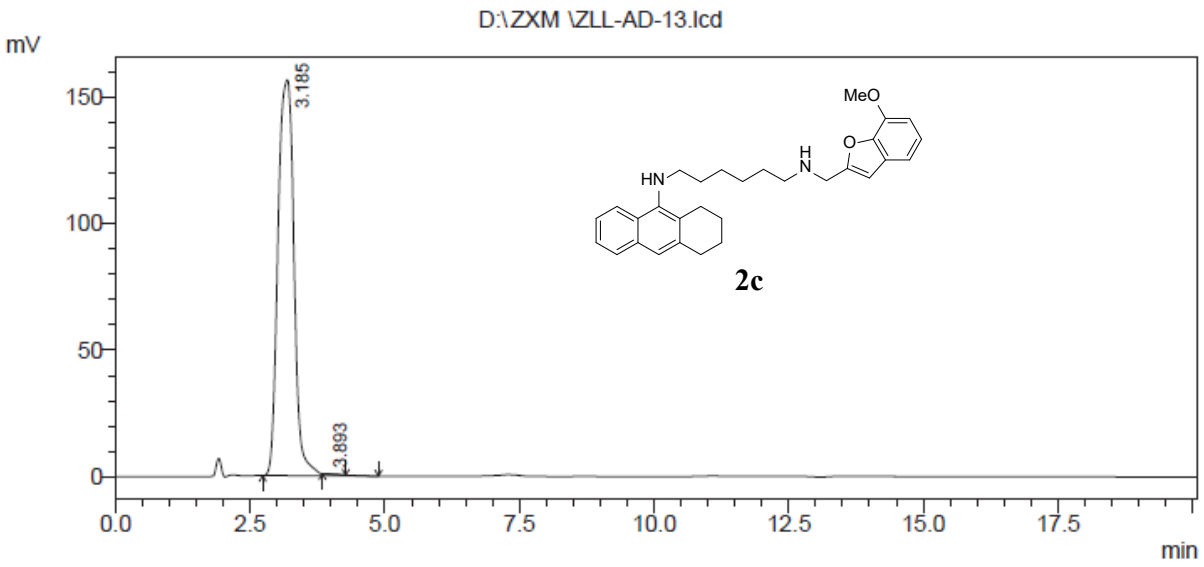

2c

Peak Table

Detector A Ch1 254nm

Peak#	R.T.	Area	Height	Area %	Height %
1	3.185	3242028	156271	99.931	99.930
2	3.893	2241	110	0.069	0.070
Total		3244269	156381	100.000	100.000

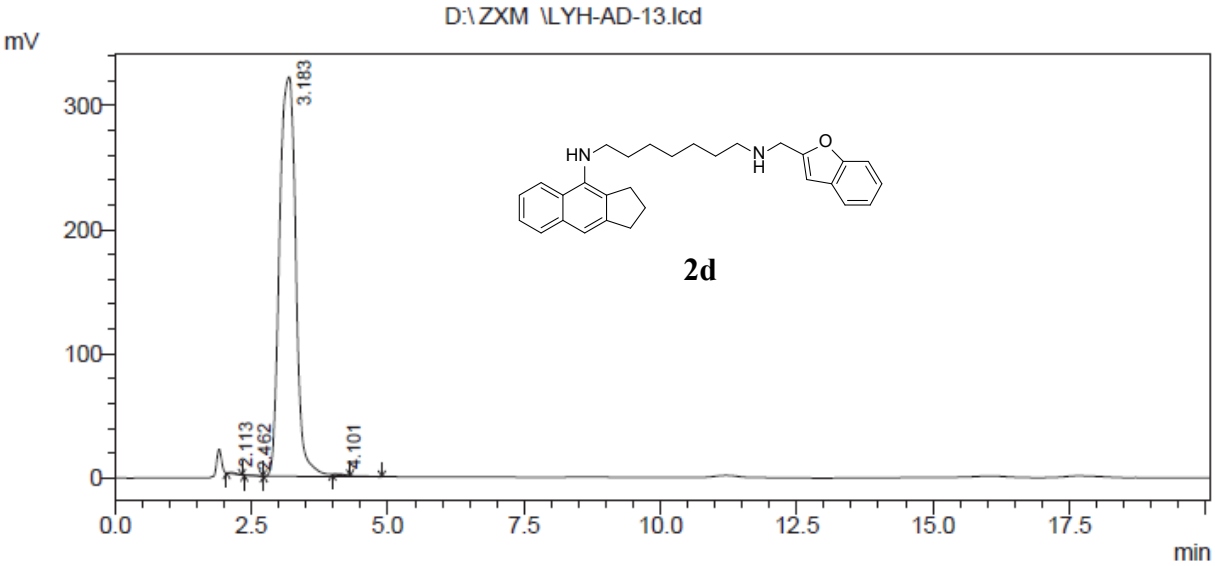

2d

Peak Table

Detector A Ch1 254nm

Peak#	R.T.	Area	Height	Area %	Height %
1	2.113	9265	926	0.138	0.286
2	2.462	3229	380	0.048	0.118
3	3.183	6704179	321610	99.701	99.345
4	4.101	7626	814	0.113	0.251
Total		6724299	323730	100.000	100.000

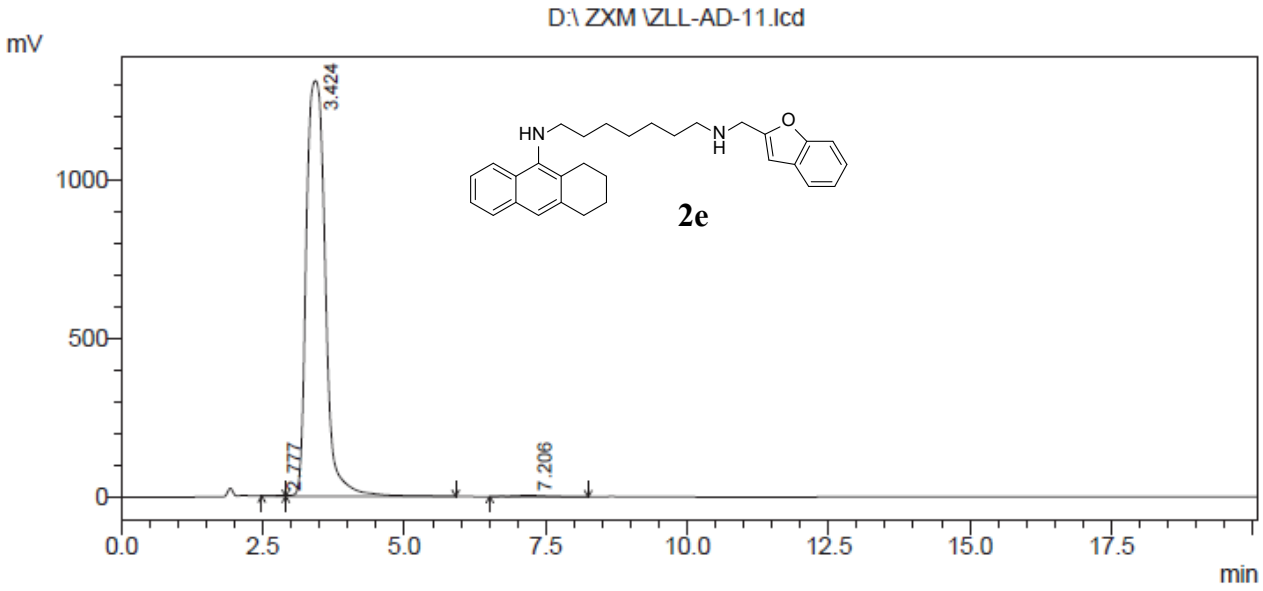

Peak Table

Detector A Ch1 254nm

Peak#	R.T.	Area	Height	Area %	Height %
1	2.777	27191	1619	0.088	0.123
2	3.424	30571401	1312924	99.466	99.601
3	7.206	136926	3639	0.445	0.276
Total		30735518	1318182	100.000	100.000

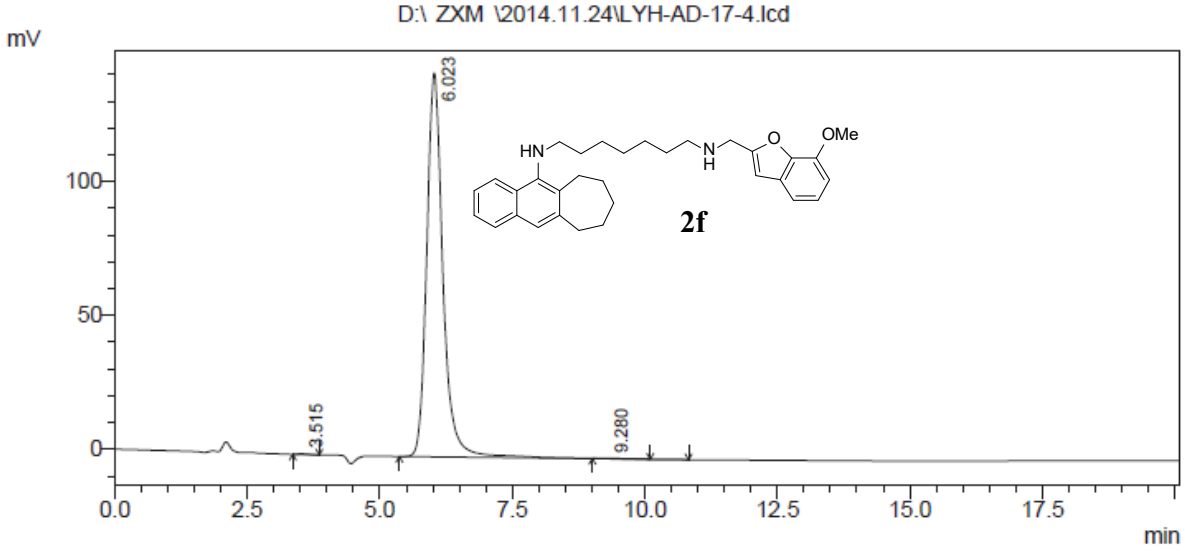

Peak Table

Detector A Ch1 254nm

Peak#	R.T.	Area	Height	Area %	Height %
1	3.515	3875	285	0.126	0.198
2	6.023	3062066	143301	99.671	99.650
3	9.280	6239	217	0.203	0.151
Total		3072180	143803	100.000	100.000

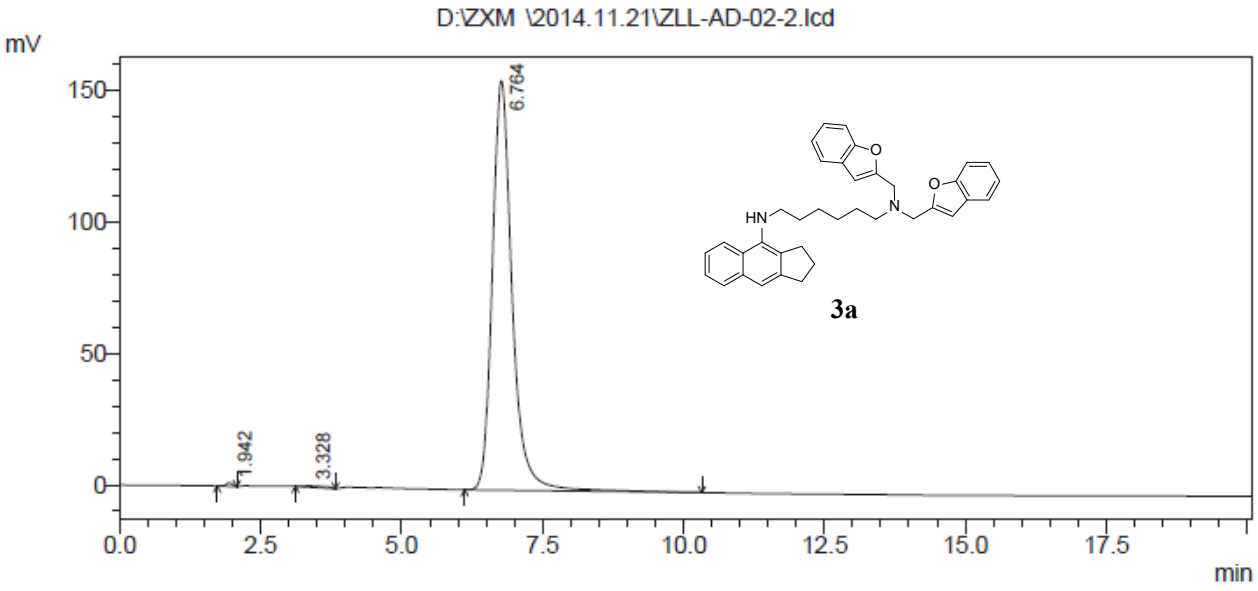

3a

Peak Table

Detector A Ch1 254nm

Peak#	R.T.	Area	Height	Area %	Height %
1	1.942	11033	1425	0.287	0.903
2	3.328	16842	491	0.438	0.311
3	6.764	3817871	155881	99.275	98.786
Total		3845746	157798	100.000	100.000

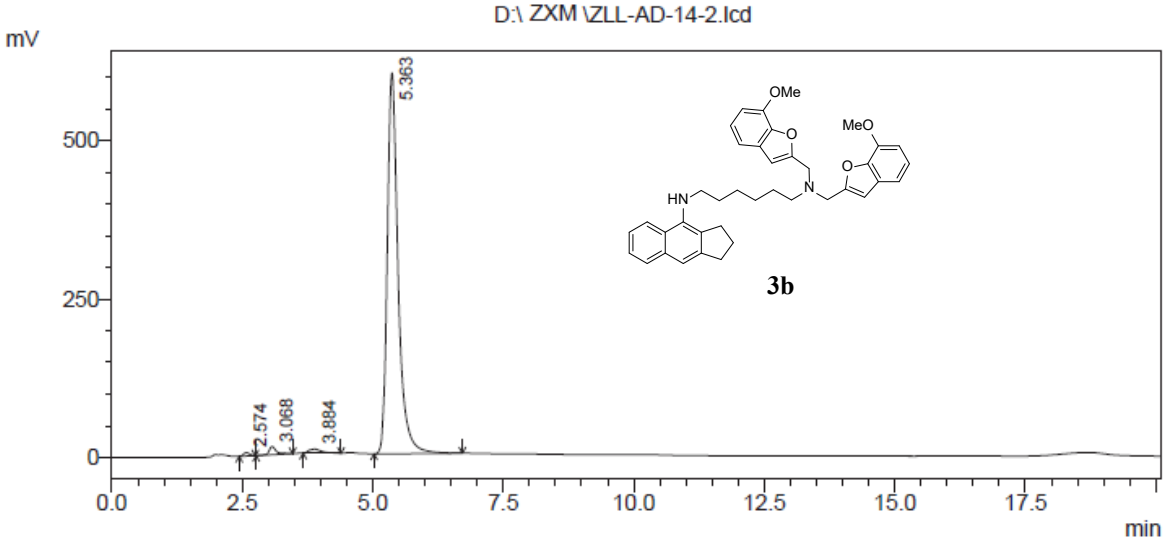

3b

Peak Table

Detector A Ch1 254nm

Peak#	R.T.	Area	Height	Area %	Height %
1	2.574	43788	5440	0.488	0.869
2	3.068	129142	12967	1.440	2.072
3	3.884	111060	6777	1.238	1.083
4	5.363	8683745	600748	96.833	95.977
Total		8967734	625932	100.000	100.000

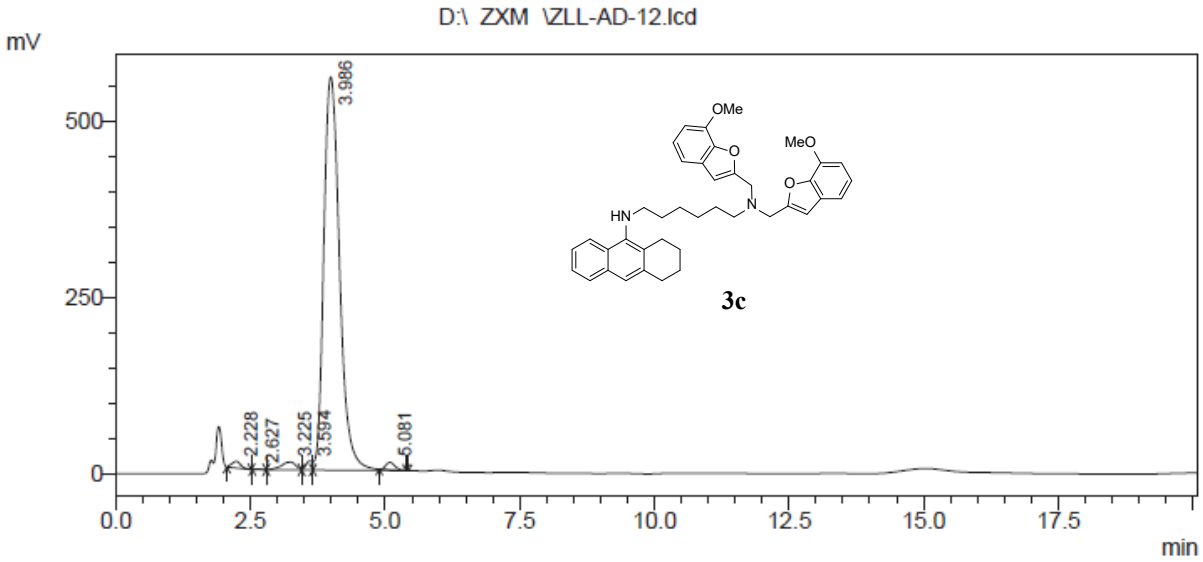

3c

Peak Table

Detector A Ch1 254nm

Peak#	R.T.	Area	Height	Area %	Height %
1	2.228	107337	9625	0.899	1.595
2	2.627	4707	629	0.039	0.104
3	3.225	206567	11124	1.731	1.844
4	3.594	107244	12799	0.899	2.122
5	3.986	11383529	558391	95.393	92.563
6	5.081	123955	10688	1.039	1.772
Total		11933340	603256	100.000	100.000

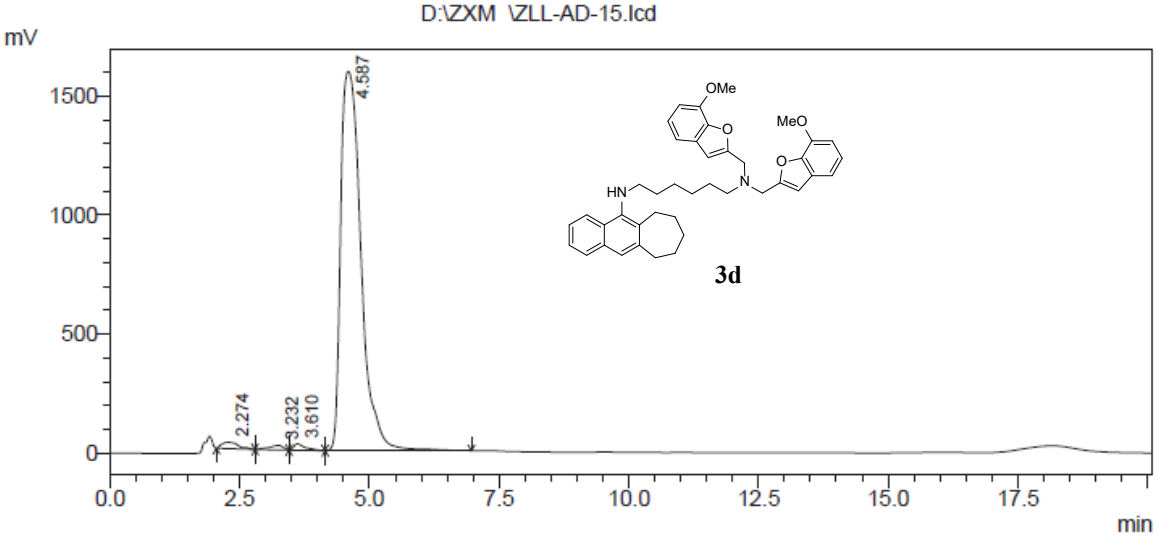

3d

Peak Table

Detector A Ch1 254nm

Peak#	R.T.	Area	Height	Area %	Height %
1	2.274	606940	26958	1.357	1.619
2	3.232	360952	18535	0.807	1.113
3	3.610	414984	26935	0.928	1.617
4	4.587	43359054	1592993	96.909	95.651
Total		44741930	1665421	100.000	100.000

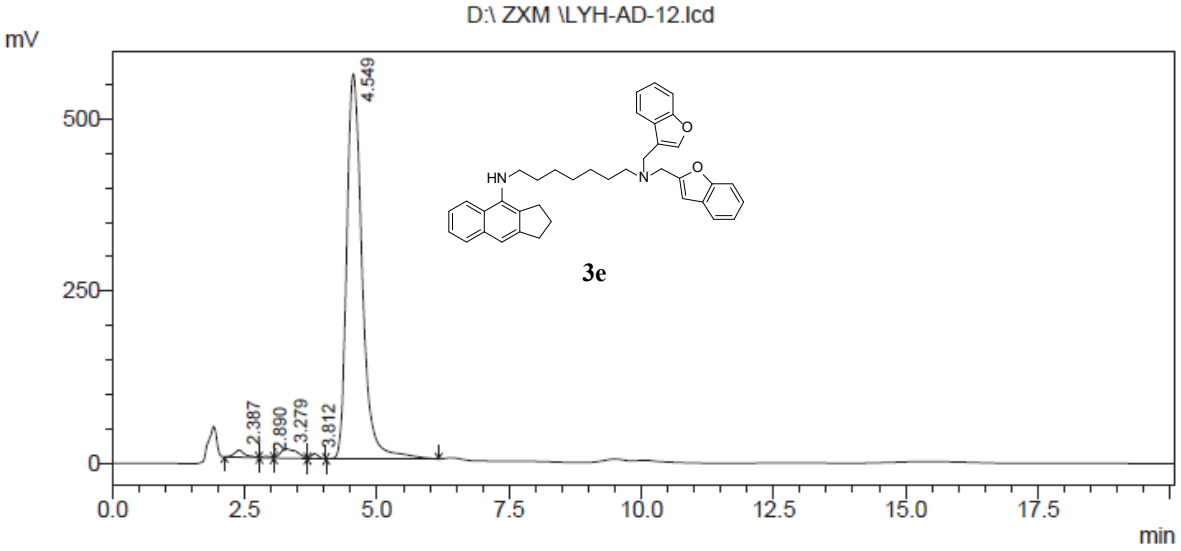

3e

Peak Table

Detector A Ch1 254nm

Peak#	R.T.	Area	Height	Area %	Height %
1	2.387	143824	10349	1.209	1.745
2	2.890	25546	2448	0.215	0.413
3	3.279	296277	13771	2.491	2.322
4	3.812	69841	7411	0.587	1.250
5	4.549	11359445	558955	95.498	94.269
Total		11894933	592934	100.000	100.000

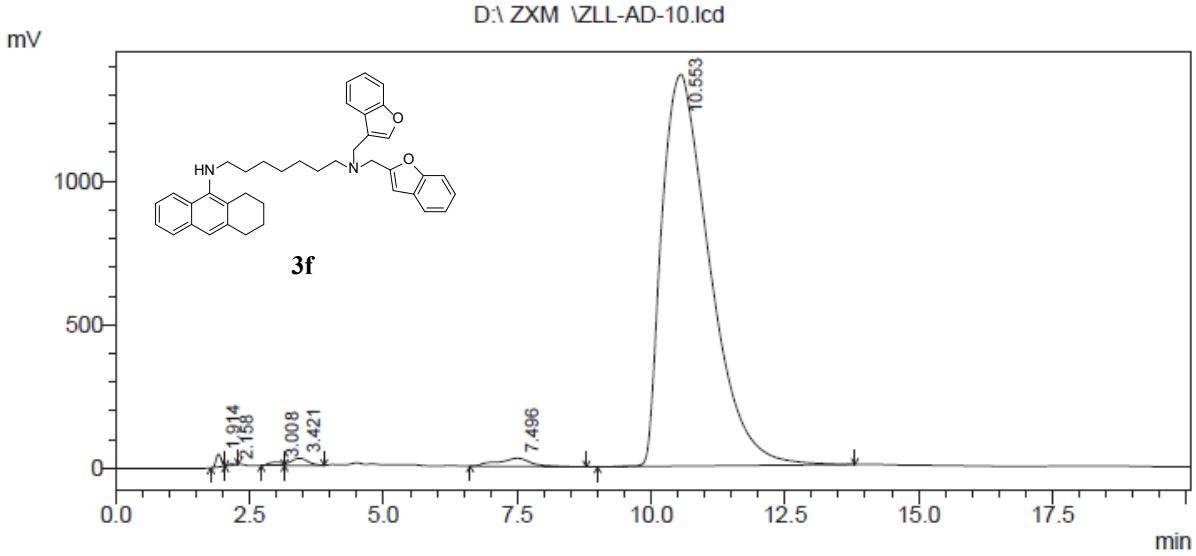

3f

Peak Table

Detector A Ch1 254nm

Peak#	R.T.	Area	Height	Area %	Height %
1	1.914	301397	45045	0.347	3.047
2	2.158	44072	4646	0.051	0.314
3	3.008	209063	11981	0.241	0.810
4	3.421	556046	24535	0.641	1.659
5	7.496	1266154	28701	1.460	1.941
6	10.553	84365822	1363682	97.260	92.228
Total		86742555	1478590	100.000	100.000

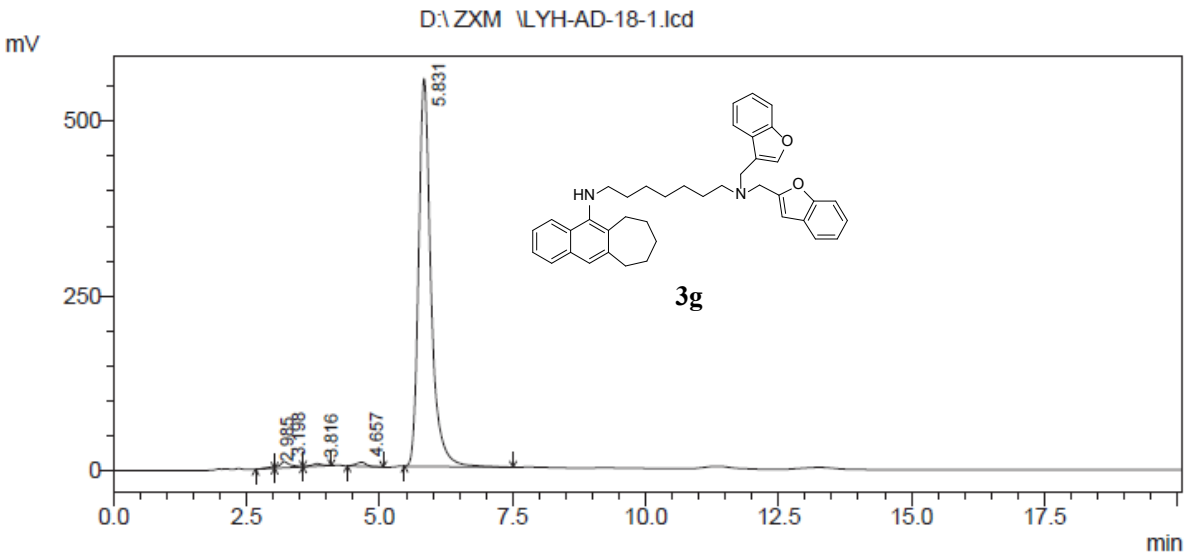

Peak Table

Detector A Ch1 254nm

Peak#	R.T.	Area	Height	Area %	Height %
1	2.985	27287	2336	0.294	0.405
2	3.198	122429	8973	1.318	1.556
3	3.816	50756	3611	0.547	0.626
4	4.657	84197	6170	0.907	1.070
5	5.831	9000873	555631	96.934	96.343
Total		9285541	576722	100.000	100.000

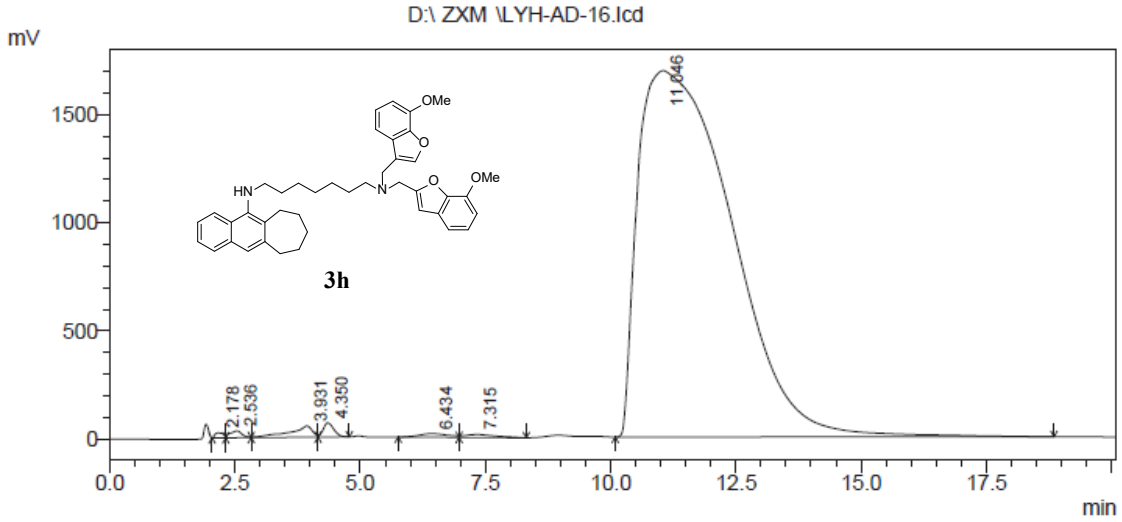

Peak Table

Detector A Ch1 254nm

Peak#	R.T.	Area	Height	Area %	Height %
1	2.178	285235	22813	0.127	1.202
2	2.536	529706	31210	0.236	1.644
3	3.931	1651377	52017	0.735	2.741
4	4.350	966372	66410	0.430	3.499
5	6.434	659140	16651	0.293	0.877
6	7.315	587489	14050	0.261	0.740
7	11.046	219997478	1694739	97.917	89.296
Total		224676796	1897890	100.000	100.000

^{1}H NMR, ^{13}C NMR and HRMS spectra for compound N^{1}-(benzofuran-2-ylmethyl)-N^{7}-(1,2,3,4-tetrahydroacridin-9-yl)heptane-1,7-diamine (2e, original internal code ZL-AD-11):

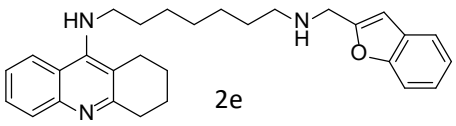

2e

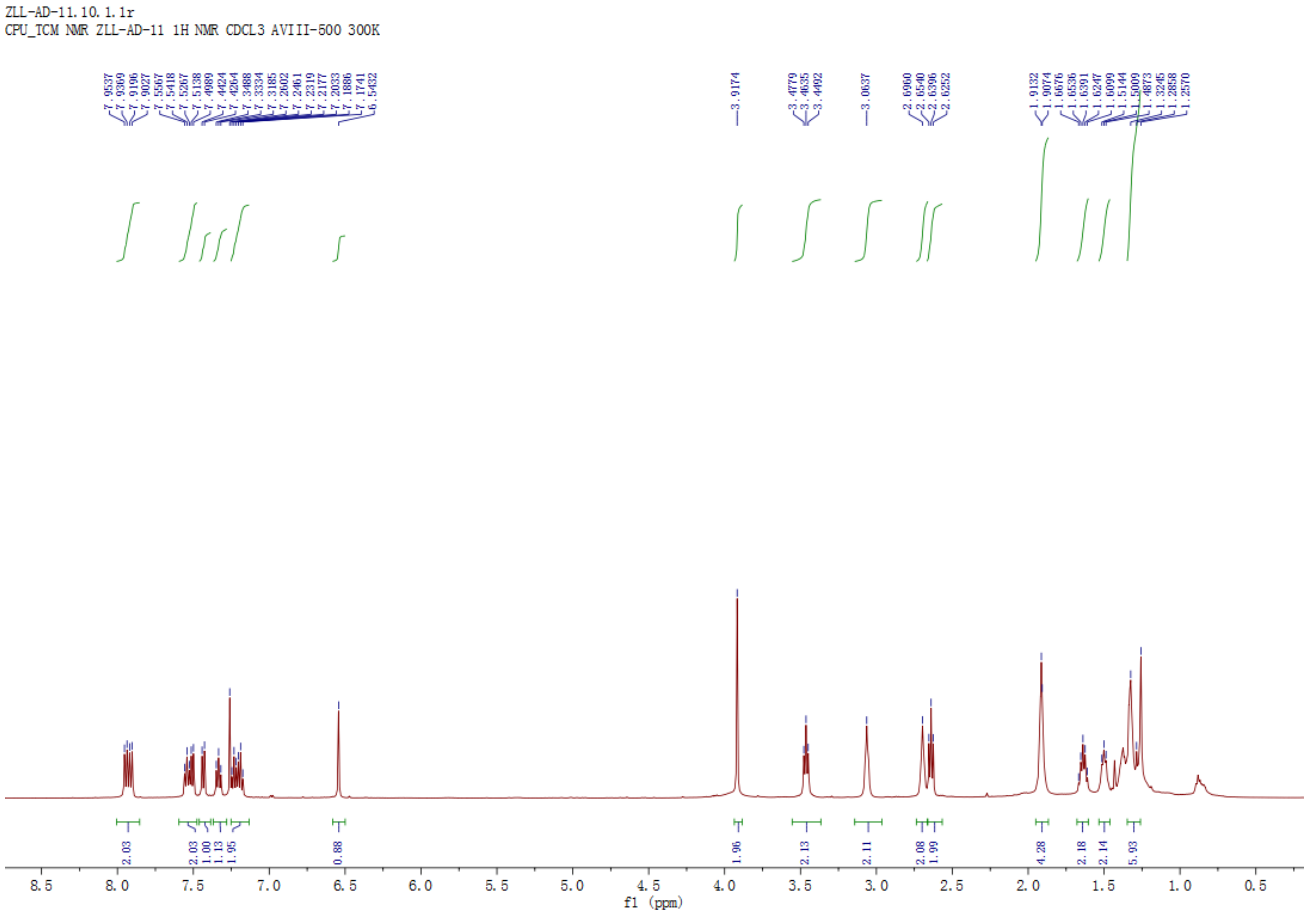

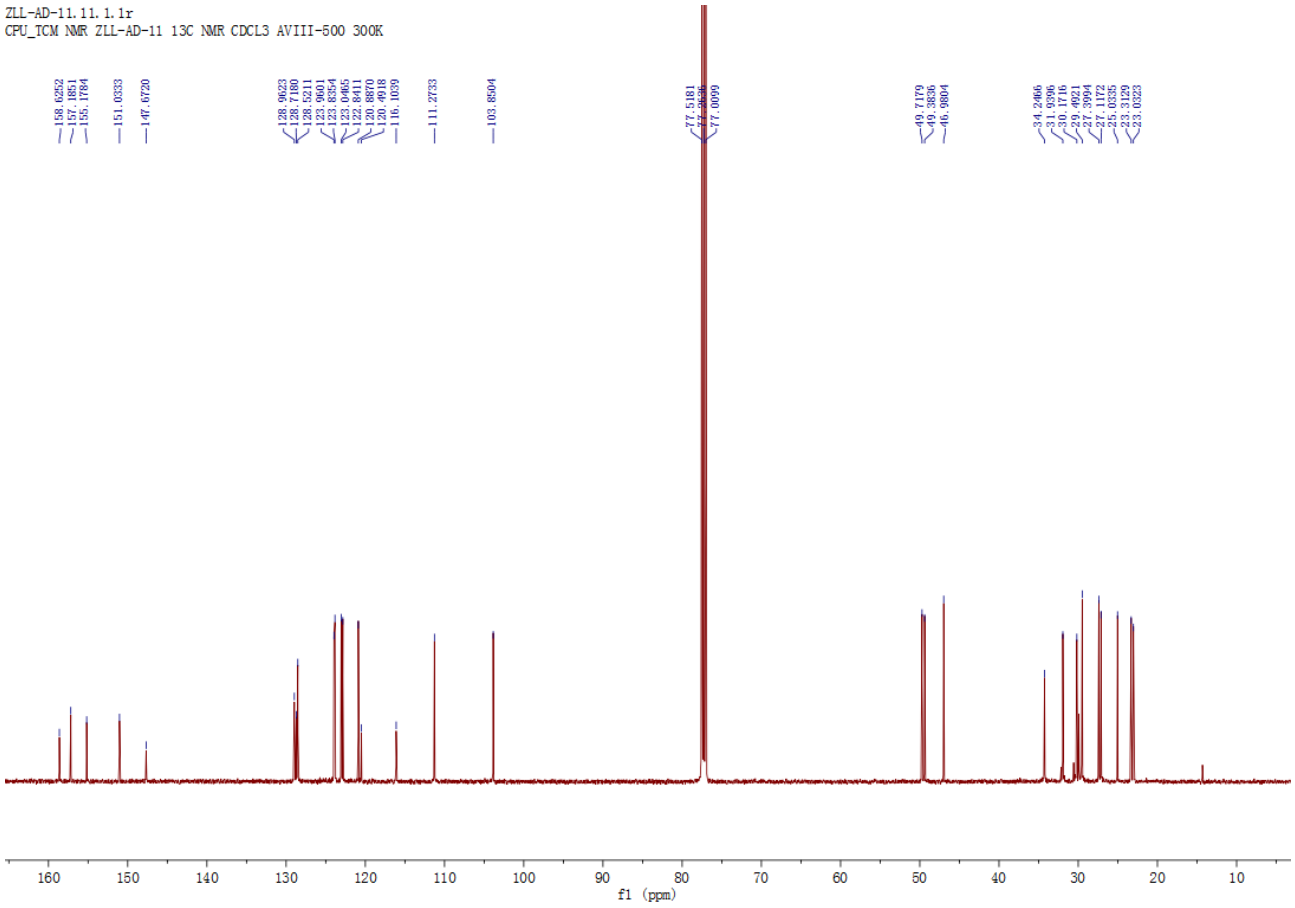
ZLL-AD-11.11.1.1r
CPU_TCM NMR ZLL-AD-11 13C NMR CDCL3 AVIII-500 300K
158.6252
157.1851
155.1784
151.0333
147.6720
128.9623
128.7180
128.5211
123.9601
123.8354
123.0465
122.8411
120.8870
120.4018
116.1039
111.2733
103.8504
77.5181
77.3060
77.0939
49.7179
49.3836
46.9804
34.2466
31.6396
30.1716
29.4921
27.3994
27.1172
25.0335
23.5129
23.0323
160
150
140
130
120
110
100
90
80
70
60
50
40
30
20
10
f1 (ppm)

Elemental Composition Report

Single Mass Analysis
Tolerance = 5.0 PPM / DBE: min = -1.5, max = 20.0
Selected filters: None

Monoisotopic Mass, Even Electron Ions
349 formula(e) evaluated with 1 results within limits (up to 50 best isotopic matches for each mass)
Elements Used:
C: 0-50 H: 0-100 N: 0-10 O: 0-5

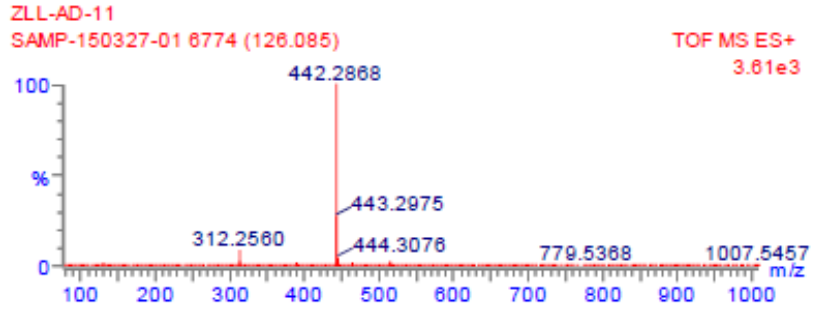

Minimum:				-1.5		
Maximum:		5.0	5.0	20.0		
Mass	Calc. Mass	mDa	PPM	DBE	i-FIT	Formula
442.2868	442.2858	1.0	2.3	13.5	38.9	C29 H36 N3 O

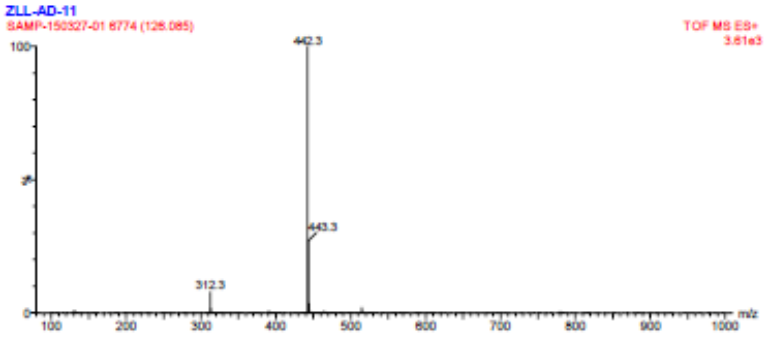

References

1. Ellman, G. L.; Courtney, K. D.; Andres, V., Jr.; Feather-Stone, R. M. A new and rapid colorimetric determination of acetylcholinesterase activity. *Biochem. Pharmacol.* **1961,** *7*, 88-95.
2. Silverman, R. B. *The organic chemistry of enzyme-catalyzed reactions*. Academic Press: San Diego, **2000**.
3. Bevc, S.; Konc, J.; Stojan, J.; Hodoscek, M.; Penca, M.; Praprotnik, M.; Janezic, D. ENZO: a web tool for derivation and evaluation of kinetic models of enzyme catalyzed reactions. *PLoS One* **2011,** *6*, e22265.
4. Bartolini, M.; Bertucci, C.; Cavrini, V.; Andrisano, V. beta-Amyloid aggregation induced by human acetylcholinesterase: inhibition studies. *Biochem. Pharmacol.* **2003,** *65*, 407-416.
5. Naiki, H.; Higuchi, K.; Nakakuki, K.; Takeda, T. Kinetic analysis of amyloid fibril polymerization in vitro. *Lab. Invest.* **1991,** *65*, 104-110.
6. Bartolini, M.; Bertucci, C.; Bolognesi, M. L.; Cavalli, A.; Melchiorre, C.; Andrisano, V. Insight into the kinetic of amyloid beta (1-42) peptide self-aggregation: elucidation of inhibitors' mechanism of action. *ChemBioChem* **2007,** *8*, 2152-2161.
7. Denizot, F.; Lang, R. Rapid colorimetric assay for cell growth and survival. Modifications to the tetrazolium dye procedure giving improved sensitivity and reliability. *J. Immunol. Methods* **1986,** *89*, 271-277.
8. Engh, R. A.; Huber, R. Accurate bond and angle parameters for X-ray protein structure refinement. *Acta Crystallogr., Sect. A: Found. Crystallogr.* **1991,** *47*, 392-400.
9. Chen, V. B.; Arendall, W. B., 3rd; Headd, J. J.; Keedy, D. A.; Immormino, R. M.; Kapral, G. J.; Murray, L. W.; Richardson, J. S.; Richardson, D. C. MolProbity: all-atom structure validation for macromolecular crystallography. *Acta Crystallogr. D Biol. Crystallogr.* **2010,** *66*, 12-21.
10. Kleywegt, G. J. Validation of protein models from Calpha coordinates alone. *J. Mol. Biol.* **1997,** *273*, 371-376.
11. Laskowski, R. A.; Swindells, M. B. LigPlot+: multiple ligand-protein interaction diagrams for drug discovery. *J. Chem. Inf. Model.* **2011,** *51*, 2778-2786.